Design and Cost Performance of the Multistage WDM-PON Access Networks

Guido Maier, Mario Martinelli, Achille Pattavina, *Senior Member, IEEE*, and Elio Salvadori

***Abstract*—The advantages of employing passive optical architectures in the access network have been largely recognized. Particularly, recent developments in optical technologies have made the realization of wavelength division multiplexing passive optical networks (WDM PON's) feasible and cost-effective. These networks are more future-proof than conventional PON's, thanks to their intrinsic optical transparency and their extremely high transmission capacity. A very useful optical routing device, called Waveguide Grating Router, is the basic building-block of new PON architectures capable of connecting a large number of users or to improve the use of the optical bandwidth. In this paper, we analyze the connectivity of WDM PON's composed of multiple stages of WGR devices. A design tool is also presented which is able to easily evaluate the connectivity functions of complex WDM PON's. The feasibility of these architectures is discussed by considering the costs and the technological limitations on the optical components.**

***Index Terms*—Passive optical network, waveguide grating filter, wavelength routing.**

I. Introduction

THE present fast development of new broad-band telecommunication services makes the upgrading of the access infrastructure a demanding research goal. To run video as well as the advanced Internet applications even the residential customers need the availability of a channel capacity that seems hardly achievable with the traditional copper wire-based POTS access networks [25].

Different "wired" solutions for the access network are currently being developed. The most important of these solutions are the digital subscriber loop (DSL) [24], hybrid fiber coax (HFC) and fiber-in-the-loop (FITL). It is actually a very debated issue which one among these solutions will better meet the needs of the future broad-band telecommunication network, known as the B-ISDN (Broadband Integrated Services Digital Network) [21]. The FITL solution is receiving at present more attention than in the past by the telecommunication operators especially thanks to the possibility of implementing routing functions entirely by employing passive optical devices [20], [26]. In passive optical networks (PON's) a group of optical network units (ONU's) is connected to the central office (CO) by a series of optical links. The communication links interfacing the ONU's are dedicated and form the *distribution network*. The communication link on the CO side is instead shared by all the ONU's of the network and is called *feeder network*. Between feeder and distribution network a structure composed by one or more remote nodes (RN's) entirely implemented by passive optical devices (and in some cases intermediate optical links) performs the separation of downstream optical channels as well as the multiplexing of upstream optical channels in a transparent way. PON's, when compared to networks with active components, offer several advantages: low cost, high reliability, no need for maintenance. These characteristics favor the configuration called fiber-to-the-home (FTTH), in which subscribers are connected to the CO by means of all optical channels.

The time-division-multiplexed PON (TDM-PON) is the best known solution for FTTH [Fig. 1(a)] [26]: the optical carrier is shared by means of a splitter among all the subscribers. It can be implemented with low cost sources and components, but the number of users is limited by the splitter attenuation and by the working bit-rate of the transceivers in the CO and in the ONU's. In a wavelength-division-multiplexed PON (WDM-PON) [Fig. 1(b)] each subscriber is assigned a separate WDM channel; these channels are routed by passive wavelength-routing device located in the remote nodes [29], [31], [17], [16]. These networks are intrinsically transparent to the channel bit-rate, do not suffer power splitting losses and allows enhanced reliability and privacy.

In recent WDM PON's, the demultiplexing function is implemented by waveguide grating routers (WGR's) [1]. This passive wavelength routing component—also called arrayed waveguide gratings (AWG's) or PHASAR's—has been extensively studied [9], [10], [2], [8] [7], [13]. It has become the basic building blocks of WDM PON's. In most cases it is realized with silica-on-silicon technology in integrated optics (Fig. 2). The internal structure of a WGR is based on two integrated optical star couplers interconnected by an array of waveguides.

Among the best known WDM-PON's in literature are RITE-Net and LAR-Net, both proposed originally by AT&T's researchers [3], [4], though many other studies and experimental demonstrations have also been reported [28], [27], [30]. In both these networks a WGR is used in one single remote node as a routing stage. The two architectures have been realized as experimental lab testbeds; their performance has been demonstrated and the corresponding results are reported in many papers [32], [33], [18], [19], [34]. The operation of these networks with optical wideband sources has also been proposed, to overlay broadcast over switched services or to implement a low-cost switched service solution by employing the spectral-slicing technique. In this paper we will consider

Manuscript received January 26, 1999; revised October 8, 1999.

G. Maier is with CoreCom, Milan 20131, Italy (e-mail: maier@corecom.polimi.it).

M. Martinelli and A. Pattavina are with the Department of Electronics and Information, Politecnico di Milano, Milan 20133, Italy (e-mail: achille@elet.polimi.it).

E. Salvadori was with the Department of Electronics and Information, Politecnico di Milano, Milan 20133, Italy. He is now with Nokia Networks.

Publisher Item Identifier S 0733-8724(00)01309-8.

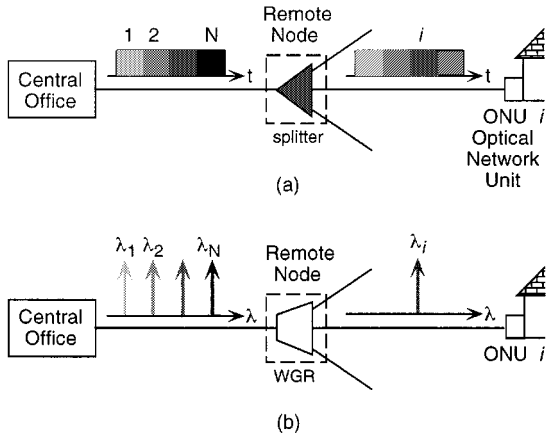

Fig. 1. FTTH network architectures: (a) TDM-PON and (b) WDM-PON.

only the case of WDM-PON's employing narrowband optical sources (lasers) for switched services.

In the two AT&T networks, different multiplexing techniques are used to implement the bidirectional transmission. In LAR-Net, one single fiber is dedicated to every subscriber: the downstream traffic is transmitted employing wavelengths belonging to the 1550 nm optical window, while for upstream traffic the wavelengths in the 1300 nm window are used (WDM "coarse" bidirectionality). In RITE-Net, two fibers are dedicated to every subscriber, each able to carry the traffic in one direction (space division bidirectionality).

These architectures seem to suffer from two main limitations:

1) difficulty in scaling the number of ONU's once the network is laid down;
2) limited number of users, because the fabrication technology imposes limitations on the WGR size.

In an attempt to overcome these limitations in this work, we will examine some possibilities offered by the routing properties of WGR's (Section II). By exploiting these properties we will find rules that allow one to design WDM-PON architectures based on the cascading of multiple WGR stages such that the reuse of a given wavelength for more than one subscriber is possible (Section III). The final purpose will be to find criteria to obtain scalable WDM-PON's architectures with minimum cost. In order to achieve this goal we have developed an algorithm to generate various combinations of network parameters under topological and technological bounds in order to compare their costs evaluated according to suitably defined cost functions (Section IV). Finally a tool is presented based on a matrix representation of the routing functions to easily study the connectivity of WDM PON networks (Section V). We will apply this tool to the minimum cost architectures identified by cost comparison and we will discuss their technological feasibility.

II. Properties of Cascaded WGRs: Wavelength Reuse and Space Demultiplexing

In order to study and define the connectivity properties of the WGR in our work it is convenient to consider optical channels routed by a specific WGR as belonging to a discrete bidimensional domain, the two axes representing space and wavelength.

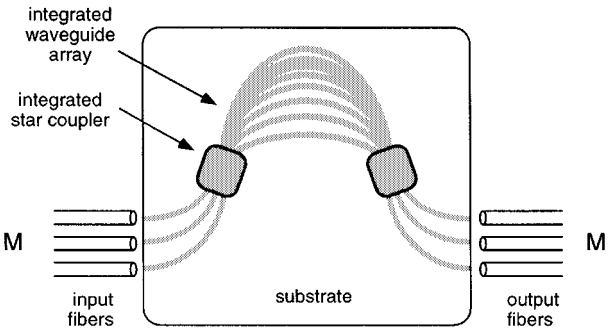

Fig. 2. Scheme of a waveguide grating routing (WGR) device.

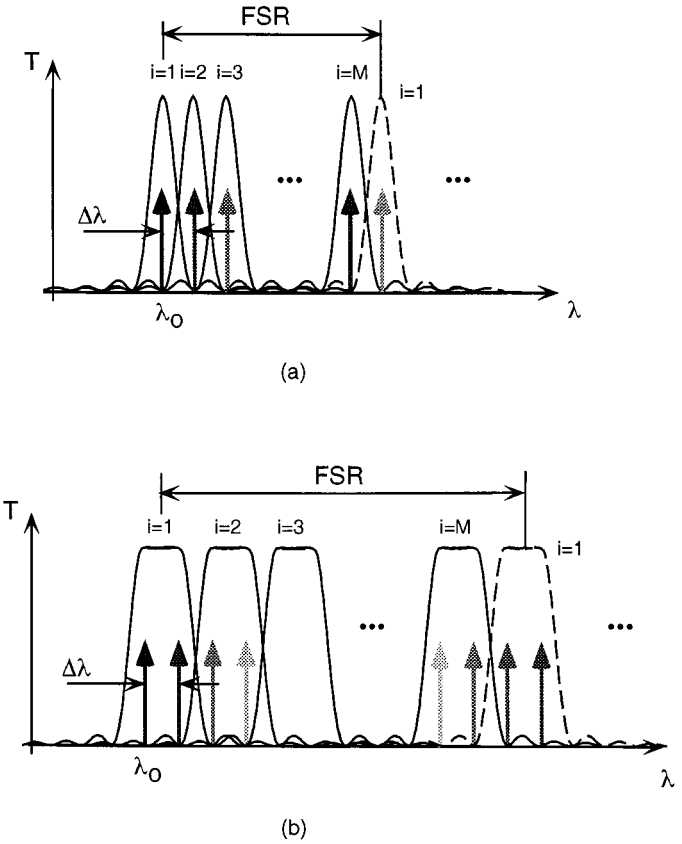

Fig. 3. Transfer function from all the inputs to output port 1 of a WGR with coarseness: (a) $C = 1$ and (b) $C = 2$.

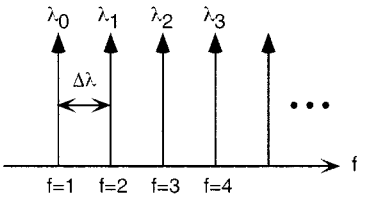

Fig. 4. Discrete wavelength domain in a WDM-PON based on WGR's.

It should be noted that the WGR, being a passive device, is able to perform space permutations, while it does not alter the wavelength of the signals. A channel in a WGR is identified therefore by two space coordinates which correspond to the input and the output port number of the WGR through which the channel enters and leaves the device. The ports are numbered by

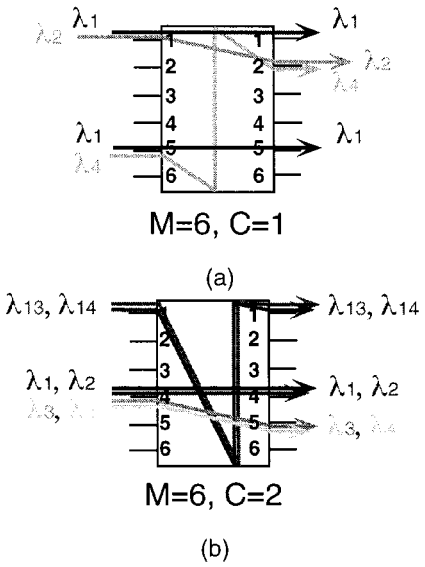

Fig. 5. Examples of routing performed by WGR's with $M = 6$ and coarseness: (a) $C = 1$ and (b) $C = 2$.

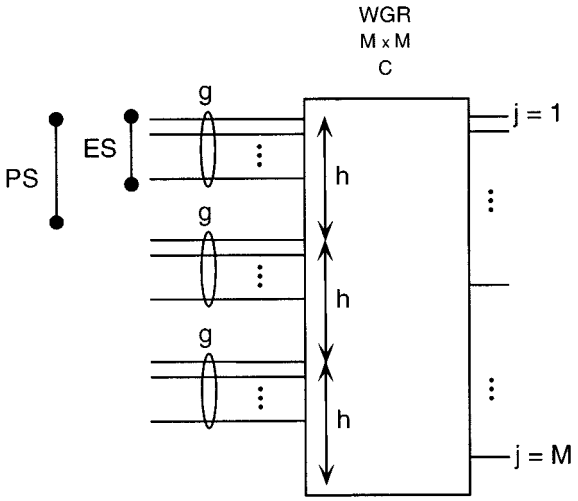

Fig. 6. Potential sets and effective sets in an input port occupancy pattern.

a progressive integer index. Since we will consider only symmetrical devices, the space coordinates can assume all the integer values from 1 to M, where M is the parameter defining the size of the WGR, i.e., the number of its input and output ports. The wavelength coordinate of the bidimensional domain can also assume discrete values. The WGR is an optical device based on interferential optical phenomena, and therefore it has a periodic behavior in the wavelength domain [13]. Upon the optical signals entering from a given input i and routed to a given output j, the WGR behaves like a passing-band periodical filter, its power transfer function having peaks repeating at a fixed wavelength interval called free spectral range (FSR). The transfer function from the input $i+1$ to a given output j has the same shape as the previous transfer function of input i, but it is shifted on the wavelength axis by a wavelength interval $\Delta\lambda$. Another shift of $\Delta\lambda$ separates this second transfer function from the transfer function between the next input $i+2$ and the output j, and so on. The WGR can be designed so that [11]

$$\mathrm{FSR} = M\Delta\lambda$$

The above equation is actually an idealization. In the reality FSR has a more complicated expression and is not exactly constant, but varies along the λ axis [12]. The following discussion is based on the idealized WGR model. We will consider again the nonideality in Section VI.

The overall transfer function of the WGR from all the inputs to a certain output is represented in Fig. 3(a).

If we consider the transfer function from an input i to an output with the same index i we can choose the wavelength corresponding to one of its peaks to be the base wavelength λ_o of the WGR. We are therefore able to specify the wavelength domain for the optical channels routed by the WGR as a discrete set of wavelengths numbered by an index f that can assume all the integer values from 1 to (theoretically) infinity.[1] This set represents a wavelength comb in which λ_o corresponds to $f = 1$ and all the subsequent wavelengths are spaced by a wavelength interval $\Delta\lambda$:

$$\lambda(f) = \lambda o + (f-1)\Delta\lambda \quad \forall f \in [1,\infty]$$

In this work, we assume that in a WDM-PON all the WGR's are tuned to the same λ_o. For this reason the wavelength domain defined for one single WGR can be extended to the entire network. Fig. 4 shows the defined discrete wavelength domain.

Thanks to specific design techniques, WGR's can be fabricated which are able to act on a "dense" comb of wavelengths, routing more contiguous wavelengths of the comb as if they were a single one [see Fig. 3(b)]. We therefore introduce a second parameter to characterize a WGR. This parameter is called coarseness C and represents the number of contiguous wavelength channels belonging to the wavelength comb (i.e. spaced by an interval $\Delta\lambda$) routable on the same output port. The coarseness corresponds to the optical resolution of the device [15].

The fabrication of this type of devices is critical (we will comment on this point later on in Section VI), basically because very flat passing-bands and very sharp transition slopes are required in the transfer function not to introduce unequal attenuation for the different optical channels.

In conclusion, a WGR characterized by size M and coarseness C operates on an optical signal belonging to its associated space-wavelength domain (i,j,f), with: $(i,j) \in [1,M]$ and $f \in [1,\infty]$, where i, j and f represent respectively the input port, the output port and the wavelength. The WGR routing function can thus be defined as [15]

$$j = 1 + \left(i - 1 + \left\lfloor \frac{f-1}{C} \right\rfloor\right) \bmod M \qquad i,j \in [1,M] \quad \text{and} \quad f \in [1,\infty] \tag{1}$$

[1]We choose to consider only wavelengths longer than λ_o. An equivalent approach would also be possible in which λ_o is chosen as the central wavelength of the wavelength domain. In this case f should range also on negative values.

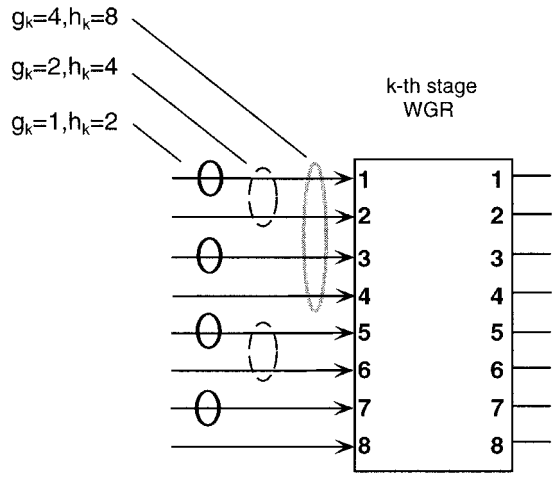

Fig. 7. Examples of input port occupancy patterns of a WGR.

The modulo-M division in (1) is a consequence of the periodical behavior of the device (FSR). We call this important property "cyclic routing."

Fig. 5(a) shows how the wavelengths λ_1 and λ_2 entering the WGR on ports 1 are routed to ports 1 and 2, respectively. The example shows that the wavelengths can be reused without collision provided they enter from different input ports: this is another one of the main properties of the WGR. Fig. 5(a) also shows the routing of wavelengths λ_4 from port 5 to output port 2. In Fig. 5(b), the routing of a WGR with $C = 2$ is reported.

On the basis of the routing properties of the WGR's we are now going in this section to find some rules to properly evaluate the WGR parameters in the various stages of a multistage WDM-PON.

We will consider the case of a WGR in which only some of its inputs are used. Under this circumstance the routing scheme of a WGR is determined by the specific choice of the input port occupancy pattern, i.e. the subset of input ports which are connected by fibers to devices belonging to the previous stage.

Let us consider a generic WGR with size M. We then subdivide the M input ports into groups of h adjacent ports. We call such groups the potential sets (PS's). To restrict our discussion to only regular topologies, we assume that h is a submultiple of M. We further consider the case when for each PS only the first g adjacent ports are used, as represented in Fig. 6. We call the used g adjacent ports the effective set (ES).

We introduce now the parameter I, which is the total number of used input terminations. I is given by

$$I = \frac{gM}{h} \tag{2}$$

Fig. 7 shows three examples of input port occupancy patterns, with $I = 4$: $g = 2, h = 4$ (sketched circle), $g = 1, h = 2$ (dark circle), $g = 4, h = 8$ (bright circle). The input ports connected in the three cases are respectively: 1, 2 and 5, 6; 1, 3, 5, and 7; 1, 2, 3, and 4.

The generic used input port i in an input pattern can be expressed as follows:

$$i = x + h(y-1) \quad x \in [1, g], \quad y \in \left[1, \frac{M}{h}\right] \tag{3}$$

where x and y indicate respectively the position of the port into its ES and the position inside the WGR of the PS it belongs to.

Substituting (3) in (1) we obtain

$$j - 1 = \left[x - 1 + (y-1)h + \left\lfloor \frac{f-1}{C} \right\rfloor\right] \bmod M \tag{4}$$

which can be solved in terms of the parameter α

$$\alpha = x - 1 + (y-1)h + \left\lfloor \frac{f-1}{C} \right\rfloor$$

as

$$\alpha = j - 1 + qM \quad q \in [0, \infty]. \tag{5}$$

From the previous equations we can now evaluate the set of all the wavelengths that, being inserted into the WGR from any of its used input ports, reach a given output port j. Substituting α into (5), we obtain

$$f = qMC - (x-1)C - (y-1)hC + (j-1)C + c \quad c \in [1, C]. \tag{6}$$

The two particular limiting cases are important for our purposes: when the ES's are composed of one single port (*Case a*) and when there is only one PS composed of all the ports of the WGR (*Case b*). That is, we have the following.

1) *Case a*: $g = 1$ and therefore from (2): $h = M/I$ ($g = 1$, $h = 2$ in the example of Fig. 7);
2) *Case b*: $h = M$ and therefore from (2): $g = I$ ($g = 4$, $h = 8$ in the example of Fig. 7).

A. Case a

We can rewrite (6) for this case, in which $x = 1$

$$f = qMC - (y-1)hC + (j-1)C + c \quad y \in [1, I]; \quad c \in [1, C]. \tag{7}$$

Let us assume that a comb of contiguous wavelengths is fed to each of the I used input terminations. The set of wavelengths which satisfy (7) is shown in Fig. 8, which displays various periodical behaviors.

Consider the output $j = 1$. In the wavelength discrete domain, moving from short to long wavelengths, we encounter a first packet of adjacent channels which come from the input belonging to the first PS. This packet contains a number of wavelength channels given by the coarseness C of the WGR. Each channel inside the packet is indexed by the number c in (7). The second packet of contiguous wavelengths we encounter comprises channels coming from the last PS and is separated from the first packet by an interval hC, with $hC = (MC)/I$, by definition of I. The entire set of I packets repeats after a wavelength interval of MC. This is due to the WGR cyclic routing.

The set of wavelengths that are routed to output $j = 2$ is obtained by shifting the set routed to $j = 1$ by a wavelength interval C.

Finally, on the output port $j = h + 1$ we find the same set of wavelengths that exits from output $j = 1$. This time, however, the input ports they are coming from are different: the sequence of y appears in fact cyclically shifted clockwise by one position. The same set of wavelengths repeats again on each output $j =$

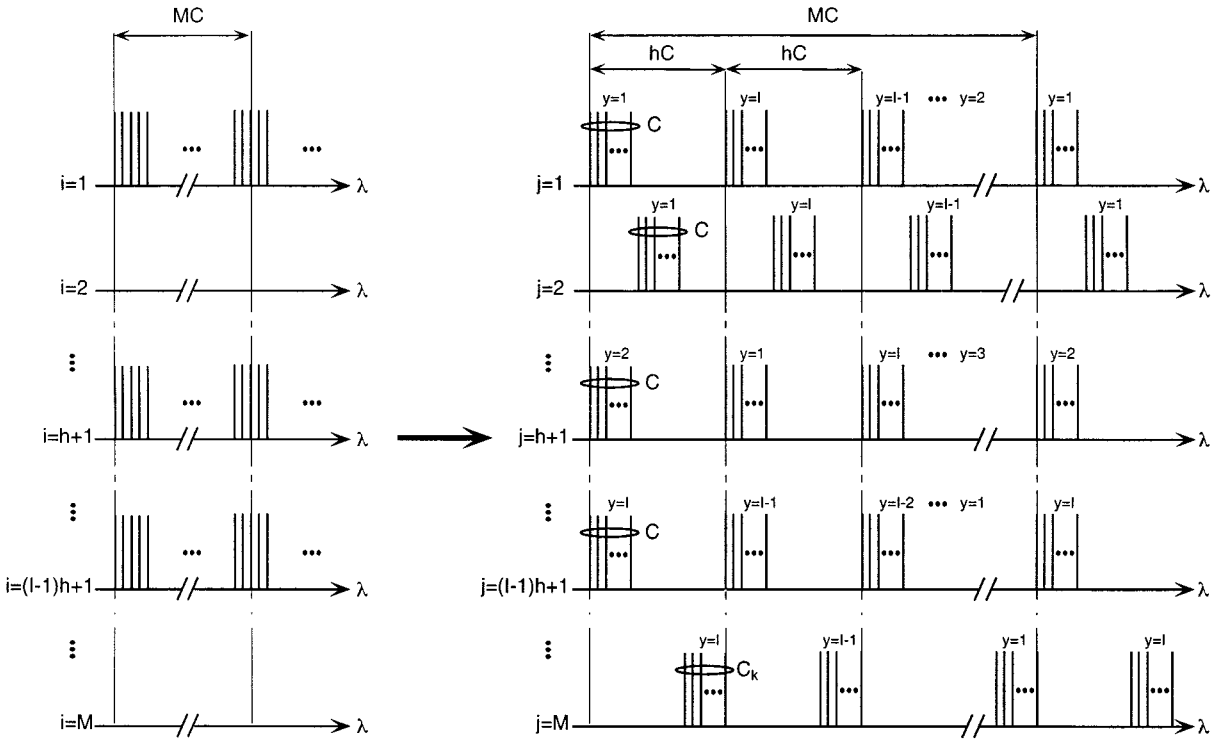

Fig. 8. Routing performed by a WGR with the input port occupancy pattern ($g = 1, h = M/I$) (*Case a*).

$\beta h+1$ ($\beta \in [0, I-1]$), every time with a clockwise shift in the input port sequence y.

The repeated presence of channels at the same wavelengths on different output ports permits wavelength reuse. This property is however typical of the WGR, no matter how the input pattern is chosen. What instead is dependent upon the choice of the input occupancy pattern (i.e., the choice of the parameters g and h), is the space demultiplexing function. The figure in fact clearly shows that each set of contiguous wavelengths coming from a used input is always spread by the WGR to different output ports. This is the condition we wanted to achieve that is fundamental to build a tree-based topology network such as the multistage WDM-PON.

Nevertheless reasoning on one single WGR is not sufficient: we must guarantee that the same space demultiplexing function can be performed also by the next downstream WGR connected to the first one. To do this we must properly chose the coarseness of the devices.

Let us suppose that the WGR described so far belongs to the stage k of a WDM-PON. The signals coming from its outputs are applied to the inputs of a WGR in stage $k+1$. We assume that the input occupancy pattern of this second device (having size M_{k+1} and coarseness C_{k+1}) is of the same type, i.e., defined by the parameters h_{k+1} and $g = 1$ (*Case a*).

Fig. 9 represents this situation. For simplicity only the first two outputs of one of the WGR's in stage k (which are identical) are shown: they are connected to the first two used inputs $i_{k+1} = 1$ (or $y_{k+1} = 1$) and $i_{k+1} = h_{k+1} + 1$ (or $y_{k+1} = 2$) of the WGR of stage $k + 1$. Two consecutive packets of wavelengths on the input of the second device, as it can be seen, are placed at a wavelength interval $h_k C_k$. If the coarseness C_{k+1} is chosen equal to this interval, independently of the size M_{k+1}, we are guaranteed that the second WGR will also perform a space demultiplexing function.

In conclusion we found a rule which allows to recursively dimension the coarseness of the WGR's in a multistage WDM-PON starting from the first stage and going downstream. Requiring that $h_k C_k = C_{k+1}$, the coarseness of a WGR of the $(k + 1)$th stage WGR's is given by

$$C_{k+1} = \frac{M_k C_k}{I_k}. \tag{8}$$

Since M_k must be of course always greater than I_k, this condition implies that $C_{k+1} > C_k$. Therefore a WDM-PON architecture built according to this scheme can be said to be of increasing coarseness (IC) type.

B. Case b

It is possible to show by a similar reasoning as for *Case a* that also with this input occupancy pattern the WGR is able to perform the space demultiplexing function. By analyzing the conditions necessary to guarantee the space demultiplexing of channels stage by stage, as we did before for *Case a*, we find the following rule:

$$C_k = \frac{M_{k+1} C_{k+1}}{I_k}. \tag{9}$$

In this second case we have the opposite situation compared to *Case a*: it can be proved that this time a WDM-PON architecture built with this rule is of decreasing coarseness (DC) type (a similar case is considered also in [15]). It should be noticed that in this case the recursive dimensioning of the coarseness must be started from the last stage.

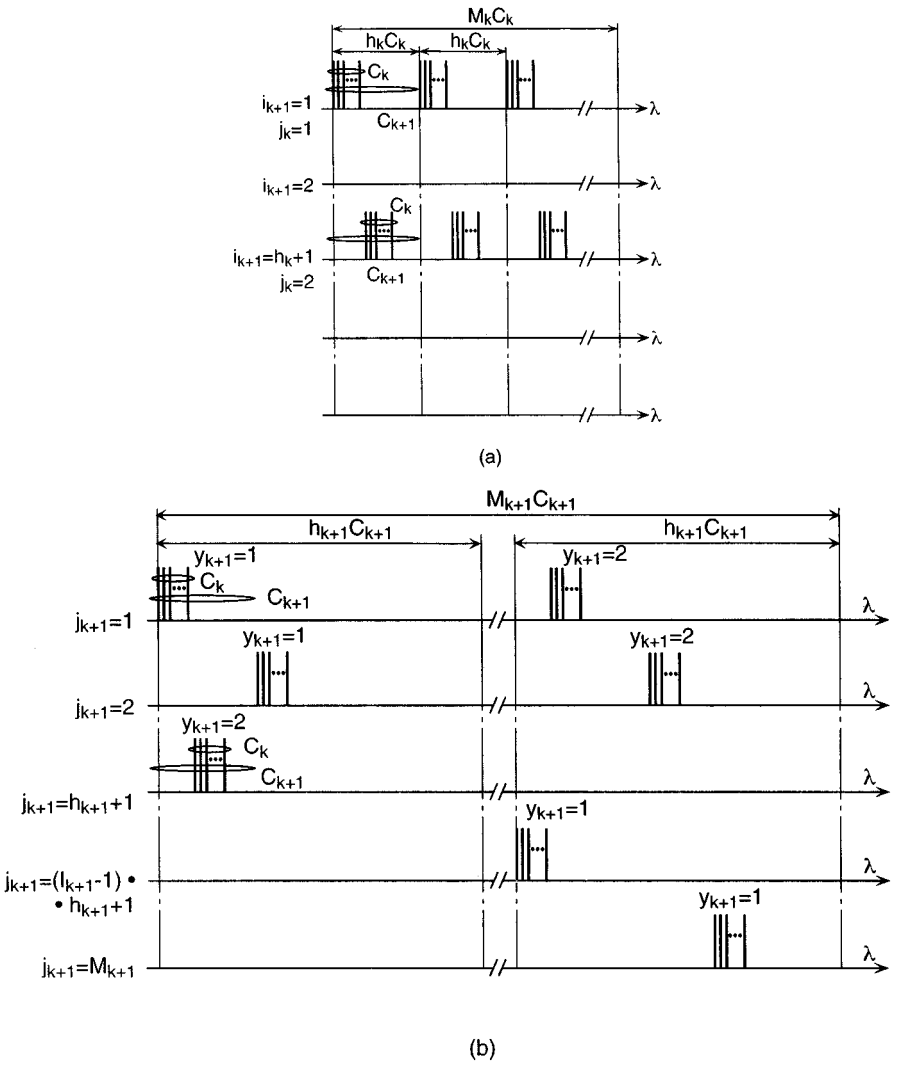

Fig. 9. Routing performed by two cascaded WGR: (a) input channels of a WGR in the stage $k+1$ when the first two outputs of the WGR of Fig. 8 placed in stage k are applied to its used input ports; (b) the resulting output channels.

C. Comparison of IC and DC WDM-PON's

Multistage IC WDM-PON's are easily scalable, while WDM-PON's of DC type do not have this property.

First of all it must be noticed that in every WGR-based WDM-PON the total bandwidth assigned to each subscriber can be flexibly increased on demand without modifying the network. This is possible thanks to the cyclic routing property of the WGR, and it can be done by adding new wavelengths to the set transmitted from the CO, suitably selected according to the periodicity of the network components. In the simple case of a single stage network, for example, with a RN of size M and coarseness $C = 1$, if the first ONU must be given an additional channel, it is sufficient to add at the CO the wavelength $f = M + 1$.

A more difficult issue is instead to expand a WDM-PON not in terms of bandwidth per user, but in terms of number of users.

In the case of an IC WDM-PON this requires to expand only those WGR's belonging to the last stage which connect the new subscribers, beside of course adding new suitably selected wavelengths to the set transmitted from the CO. Therefore the modifications to the already installed infrastructure are quite benign. This can be understood by observing that in the rule that characterizes an IC WDM-PON [see (8)] the size of a downstream WGR does not appear. It is therefore possible to modify the size of a downstream stage without changing the other parameters. An example is shown in Fig. 10.

The same is not true for a DC WDM-PON, since in (9) the parameters of a WGR of a given stage depend upon the size of the WGR's in the downstream stage. Therefore if the number of users must be expanded, the entire network must be changed.

Moreover the DC configuration is more vulnerable to WGR variations, i.e., due to temperature fluctuations along the network. In fact, the last stages, located far away from the CO and thus more subject to environmental condition variations, have small coarseness and have therefore very narrow passing bands. Even a small transfer function shift can easily suppress one channel or route it to an undesired end user. With the IC architecture only channels on the edge of the passing band face similar problems, while the relative distance of the others to the center of the passing band can fluctuate without impairment, since the transfer function is rather flat.

For these reasons regarding the scalability, we will discuss in the rest of the paper only WDM-PON network architectures with WGR coarseness increasing stage by stage, and we will not further examine the *Case b* input pattern and the DC WDM-PON's.

III. WGR Dimensioning in a Multistage WDM-PON with Increasing Coarseness

In this section we are going to apply the concepts regarding the cascading of WGR's seen in Section II for two consecutive stages to a full network structure. In the next section we will also provide a network connectivity model based on a matrix representation which allows us to evaluate the routing of every optical channel throughout the designed networks. In the last section we will discuss the feasibility of the architectures proposed taking into account technological limits concerning the required devices and power-budget system limitations.

The WDM PON architecture we are looking at is of the IC type and is composed by K cascaded stages of WGR's, with $K > 1$. The idea of cascading more stages of WGR's has been proposed in [5] and multistage architectures have been also studied in the already cited [15]. However in the former work only the case with two stages was examined in detail, while in the latter only DC WDM-PON (together with the Vernier-type WDM-PON, which we did not consider) was proposed. In our work we will instead consider the design of IC WDM-PON's with more than two stages and furthermore we will also try to find the optimal design-parameter choice for these networks.

Fig. 11 shows the architecture of a multistage WDM-PON that we are going to take as a reference in the following discussion. Without loss of generality we suppose that the WDM "coarse" bidirectionality is employed, as in LARNet. It can be shown, however, that the results obtained can be easily extended to the case when RITE-Net-like space division bidirectionality is employed.

Fig. 11 represents the schematic of a WDM-PON network connecting a number of ONU's to a single CO. The PON structure is composed of a number of stages interconnected by fiber links. Each stage is composed of passive wavelength routing devices. In the case discussed in this paper we will assume that these devices are solely WGR's and that all the WGR's belonging to a given stage have the same characteristics (size and coarseness).

Throughout this section we will use the following symbols in order to describe the network topology and to carry out the demonstration:

- U: number of users connected to a WDM PON network;
- w: maximum number of wavelengths in each link;
- K: number of WGR stages in the network;
- $\vec{N} = \{N_1, \ldots, N_k, \ldots, N_K\}$: vector containing the number N_k of WGR's composing the kth stage;
- $\vec{M} = \{M_1, \ldots, M_k, \cdots, M_K\}$: vector containing the size M_k of the WGR's composing the kth stage of the network;
- $\vec{C} = \{C_1, \ldots, C_k, \ldots, C_K\}$: vector containing the coarseness C_k of the WGR's of the stages of the network;
- $\vec{I} = \{I_1, \ldots, I_k, \ldots, I_K\}$: vector containing the number of used inputs I_k of each of the WGR's of the stage k. It represents also the total number of fibers which connect output ports of devices belonging to stage $k-1$ to a WGR of stage k.

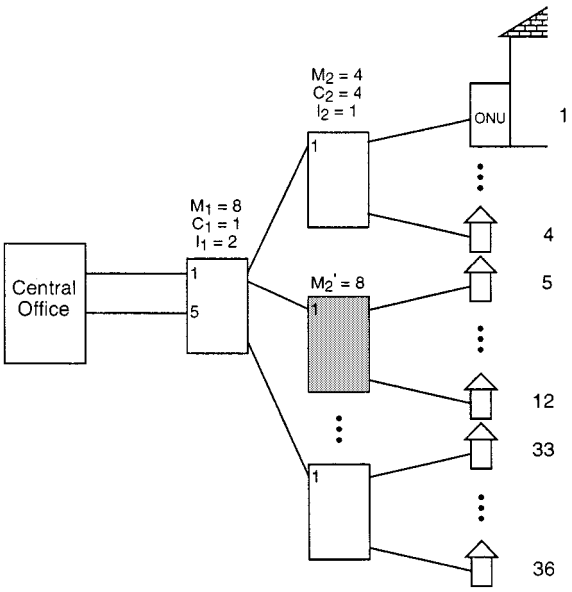

Fig. 10. Scalability of a multistage IC WDM-PON.

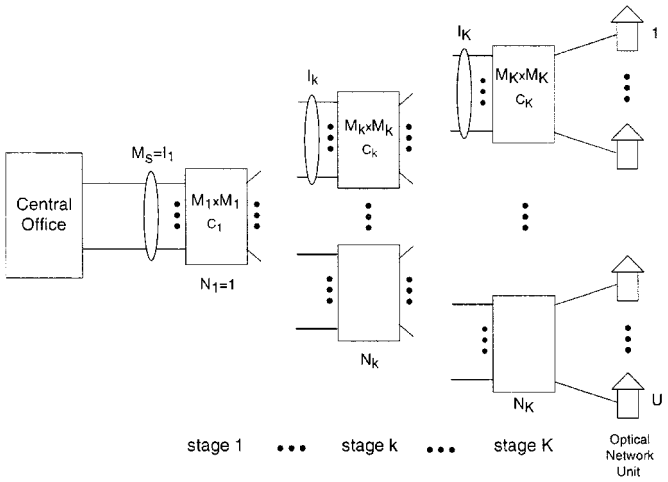

Fig. 11. Reference architecture of a multistage WDM PON.

The network structure that we are going to design is based on the following assumptions:

1) the first stage of a WDM PON network is composed of one single WGR device; thus $N_1 = 1$;
2) each output port of all the routing devices composing a certain stage (k) is either connected to an input port of a device of the following stage $(k+1)$ or to an ONU; therefore $U = M_K N_K$;
3) the coarseness of the WGR composing the first stage is $C_1 = 1$.

Since each of the N_k devices composing the stage k has only I_k input ports used, then the following condition holds:

$$N_k = \frac{M_{k-1} N_{k-1}}{I_k} \quad k \in [2, K] \tag{10}$$

which can be written as

$$I_k = \frac{M_{k-1}N_{k-1}}{N_k} \quad k \in [2, K]. \tag{11}$$

The assumption about the WGR coarseness in the first stage $(C_1 = 1)$ is necessary in an increasing coarseness WDM-PON in order to keep the parameters of the devices in the last stages in the range of the technological feasibility. By applying the condition of (8) $(C_{k+1} = (M_k C_k)/I_k)$ for a IC WDM-PON, the coarseness of second stage WGR's is given by

$$C_2 = \frac{M_1 C_1}{I_1} = \frac{M_1}{I_1}$$

The general rule is easily obtained by recursion

$$C_k = \frac{\prod_{i=1}^{k-1} M_i}{\prod_{i=1}^{k-1} I_i} \quad k \in [2, K]. \tag{12}$$

It can be noticed that this relation involves (on the right side) the elements of the vector $\vec{I}$. For purposes that will become clear shortly, we can make the following transformation. From (10) we can write, by recursion and keeping into account that $N_1 = 1$

$$N_k = \frac{\prod_{i=1}^{k-1} M_i}{\prod_{i=2}^{k} I_i} = \frac{I_1 \prod_{i=1}^{k-1} M_i}{I_k \prod_{i=1}^{k-1} I_i}.$$

By substituting the previous equation into (12), we obtain

$$C_k = \frac{N_k I_k}{I_1} \quad k \in [2, K] \tag{13}$$

which by means of (11) becomes

$$C_k = \frac{N_{k-1} M_{k-1}}{I_1} \quad k \in [2, K]. \tag{14}$$

At each stage of the network the total number of independent channels (i.e., the channels which can be separated either in wavelength or in space) must always be equal to the total number of users U. In particular, this is true at the input of the first stage, where we have the minimum number of space channels (fibers) in all the network and the maximum number of wavelengths per fiber. Here the channels are grouped in I_1 fibers, each containing a multiplex of maximum w wavelengths, so that

$$I_1 = \frac{U}{w}. \tag{15}$$

In the central office one independent transmission equipment is located for each user (so there must be U transmission equipments). However, thanks to the wavelength reuse, the effective number of laser sources can be reduced. In fact a minimum number of w optical carriers are required, which can also be produced by a single multiwavelength source. Each of these w carriers can be split with a splitting factor of I_1. A set of $I_1 w = U$ independent electrooptical modulators can then be used to encode the various downstream channels, as shown in Fig. 12.

This solution allows a sharing of the cost of the lasers (or of one single multiwavelength laser [35], [6]) by a factor I_1 (or U). But perhaps a more relevant advantage is that all the channels using a certain wavelength are encoded on a carrier generated by the same source. This implies that control of the wavelength stability in the network is much easier compared to the traditional solution in which U carriers are independently generated by different lasers [50].

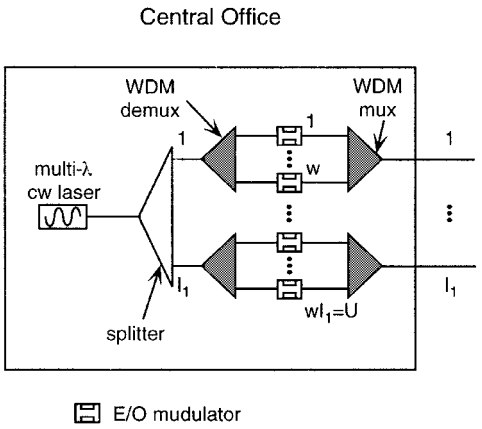

Fig. 12. A possible implementation of a CO accomplishing wavelengths reuse.

Equations (11), (14), and (15) represent the set of equations that link the design independent variables of the system w, U, $\vec{M}$ and $\vec{N}$ to the dependent variables $\vec{I}$ and $\vec{C}$.

After having identified this set of equations we can then define some bounds that the variables must respect.

An obvious bound concerns the physical connectivity of the network. The number of used inputs of any WGR must be at least one and less than the size of the device, that is

$$1 \leq I_k \leq M_k.$$

We can add another condition which prevents building WDM-PON's containing stages that do not perform any actual space demultiplexing function, but only a channel exchange on output fibers. This is achieved by requiring that in any stage the number of output ports must be strictly greater than the number of used input ports

$$I_k N_k < M_k N_k \quad \Rightarrow \quad I_k < M_k.$$

A second obvious bound stems from the definition of coarseness for a WGR

$$C_k \geq 1$$

It can be shown that the three above conditions can all be expressed by the following inequalities:

$$\max(N_k, I_1) \leq M_{k-1} N_{k-1} < M_k N_k \quad k \in [2, K]. \tag{16}$$

A last condition is necessary. We consider only networks with a tree topology. Therefore the number of devices is strictly increasing stage by stage

$$N_{k-1} > N_k \quad k \in [2, K]. \tag{17}$$

IV. Cost Comparison of IC WDM-PON Architectures

The set of equations and bounds described in Section III allows to evaluate all the possible network parameter combinations that characterize an IC WDM-PON. That is, given the number of ONU's that we must connect and the number of

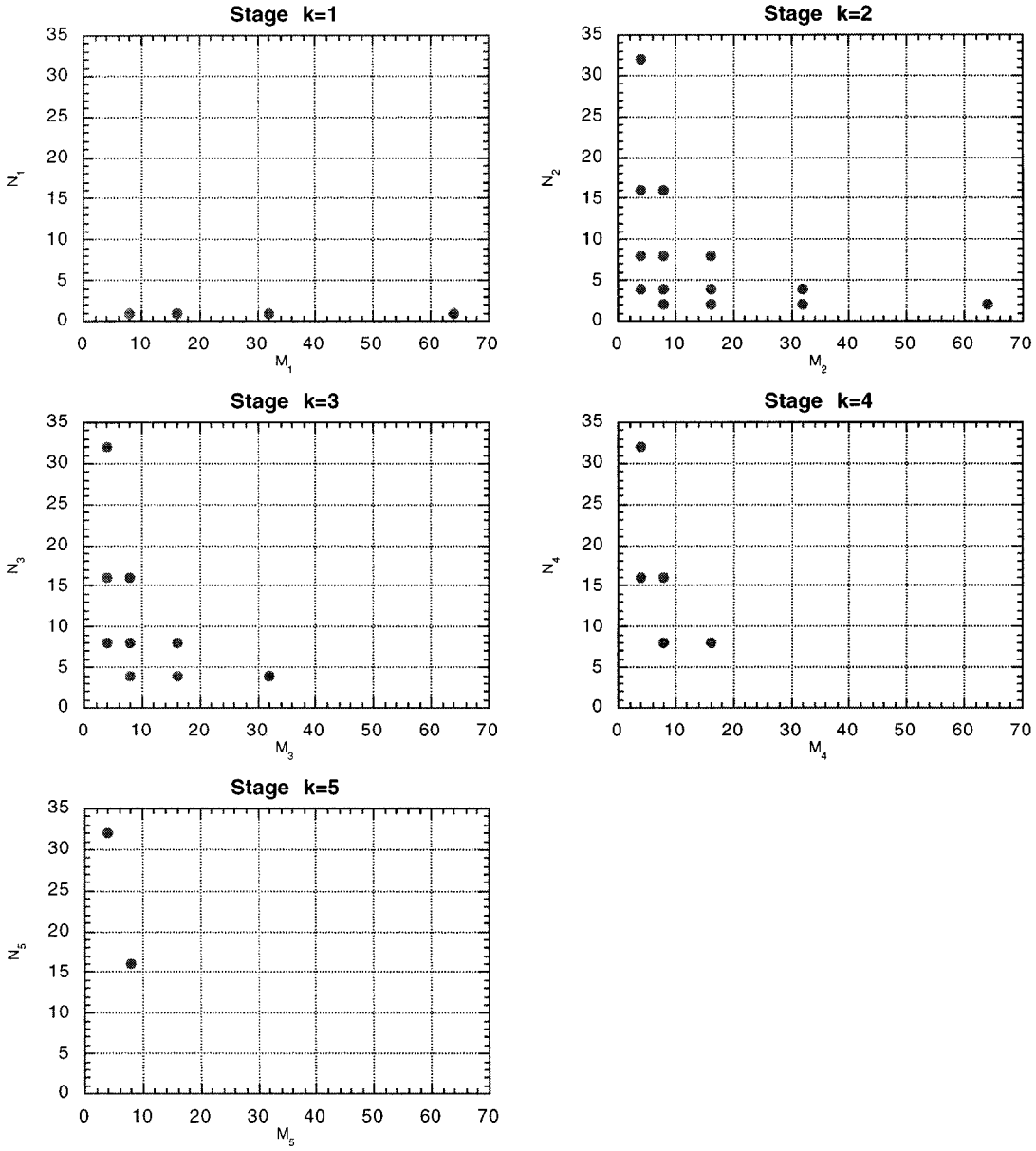

Fig. 13. Stage-by-stage plot of the values of M_k and N_k of the IC WDM-PON architectures generated for $U = 128$, $w = 32$, $M_{\max} = 64$ and $M_{\min} = 4$.

wavelengths we want to transmit from the central office, we are able to design all the possible architectures by varying the number of stages, the number of WGR's per stage and their size, the number of used inputs and the coarseness of the WGR's. Our purpose is to find out which of these combinations of parameters is optimal, i.e., minimizes the cost.

To solve the problem analytical optimization methods could be employed, like integer linear programming or other methods. As the set of possible network alternatives is relatively small we have chosen another approach, which is to generate all the possible networks and then find out the optimal parameter choice by inspection, comparing the costs.

The generation of all the possible combinations of network parameters for a given value of U and w has been performed automatically by means of a recursive algorithm. The algorithm implicitly takes into account the bounds of Section III. The only other bounds that are explicitly required are the maximum size $M_{\max}$ and the minimum size $M_{\min}$ allowable for the WGR's. The latter parameter has been added in order to avoid network architectures with too small remote nodes (such as 2×2 WGR's) that would not have much practical significance, and also in order to reduce the number of architectures which can be generated. The algorithm begins by generating the first stage of the network according to (15). Then it recursively generates the other downstream stages each time choosing a particular set of N_k and M_k which satisfy the bounds of (16) and (17), and consequently evaluating C_k and I_k, according to (11) and (14). When the algorithm reaches the last stage, it stores the architecture. Then it goes upstream one stage, changes the set of parameters for that stage and goes downstream in depth toward the last stage again. In this way, by recursion, all the possible architectures are explored.

An example of the architectures generated by the algorithm is provided in Fig. 13. The figure shows the couples (M_k, N_k)

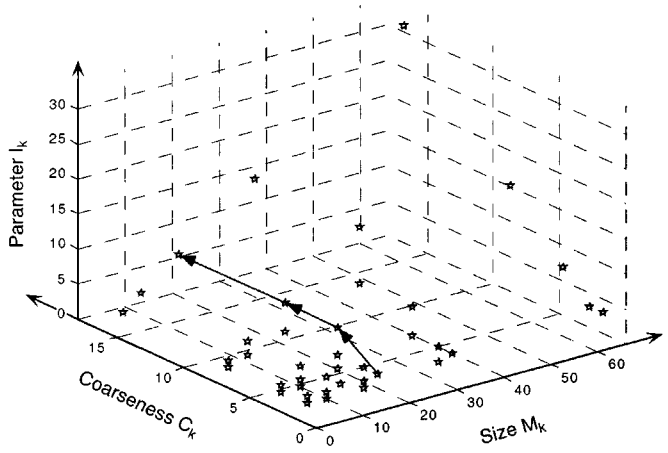

Fig. 14. Plot of the architectures generated with $U = 128$, $w = 32$, $M_{\max} = 64$ and $M_{\min} = 4$ in the space (M_k, C_k, I_k). The polygon identifies the architecture: $\vec{M} = [16\ 16\ 16\ 16]$, $\vec{N} = [1\ 2\ 3\ 4]$, $\vec{C} = [1\ 4\ 8\ 16]$, $\vec{I} = [4\ 8\ 8\ 8]$.

generated for each stage k, for $U = 128$, $w = 32$, $M_{\max} = 64$ and $M_{\min} = 4$.

Fig. 14 displays the plot of the points in the space (M_k, C_k, I_k) generated by the algorithm, given the same set of input data of Fig. 13. The polygon marked with arrows represents the network architecture: $\vec{M} = [16\ 16\ 16\ 16]$, $\vec{N} = [1\ 2\ 3\ 4]$, $\vec{C} = [1\ 4\ 8\ 16]$, $\vec{I} = [4\ 8\ 8\ 8]$.

To compare the various architectures we defined two distinct cost functions.

The first function takes into account the cost of the WGR's. We assume these devices to be fabricated in integrated optics, in silica-on-silicon technology. The cost of currently commercial devices of this kind depends mainly upon the WGR size. In fact, the coarseness of the device is determined by the particular design of the lithographic mask used to etch the shapes of the star couplers and of the integrated waveguides on the substrate. Instead the number of ports of the WGR directly affects its physical dimension, due essentially to the fixed amount of substrate area required to couple each waveguide to a fiber. Larger devices have lower fabrication yields and moreover are more difficult to be thermally stabilized; therefore their cost increases. Actually the growth is less than linear: the cost per port slightly reduces with the size.

In this study, we have considered the costs of currently (middle of 1998) commercially available devices, as summarized in Table I. All the reported costs have been provided by a manufacturer, except the last one, which has been extrapolated from the other data. It is reasonable to expect a drop of the cost of WGR manufacturing as a consequence of a production volumes increase that can happen in future as these devices will become more and more popular as building blocks of optical networks and systems. However, the assessment of an exact logistical function is beyond the scopes of this paper.

The second cost function accounts for the cable cost and their installation. We use in this case the data reported in [26] as a reference to establish the cost per kilometer (Table II). We have assumed that all the I_k fibers which feed a WGR stage k are hosted in one single cable. The cost of the cable is for simplicity considered independent of the number of fibers it can contain.

TABLE I
WGR COSTS (AT PRESENT VOLUME OF PRODUCTION)

WGR size	Cost
4	6580 $
8	8660 $
16	13320 $
32	20840 $
64	32000 $

TABLE II
CABLE AND INSTALLATION COST PER KILOMETER

Fiber cost	2000 $
Installation cost	15000 $
Total	17000 $

TABLE III
LINK LENGTHS (METER) IN MULTISTAGE WDM-PONS. LINKS ARE NUMBERED STARTING FROM THE CO AND GOING DOWNSTREAM

	Link number					
Number of WGR stages	1	2	3	4	5	> 5
1	1000	570				
2	1000	400	170			
3	1000	400	100	70		
4	1000	400	100	50	20	
> 4	1000	400	100	50	20	≈ 0

The installation cost reported in the table comprises the cost of the cable and of the trench building operation. We have also neglected the fact that partially used cables can host fibers of other parallel WDM-PONs: our cost evaluation does not take into account cable reuse (and therefore it would overestimate the costs if a global area network design with more PON's should be performed).

Of course, once the link cost per kilometer is known, the lengths of all the cable links in a multistage WDM PON must also be known to evaluate the total cost. To find this information is not an easy task, since up to now there are no commercial installations of multistage WDM-PON's. Therefore we have taken as a reference other similar but more traditional networks. Many data are available regarding TDM-PON's (two stage architectures). We suppose that the overall CO-to-ONU mean distance in a WDM-PON is 1.57 km, roughly equal to the mean overall distance of various TDM-PON testbeds, which is 1.5 km. The length of the interstage links when there are more than two stages is even more difficult to forecast. In this case we have considered as a model the access network physical architectures of the present copper-based POTS installations [51]. We suppose that the WGR's of a multistage WDM PON could be installed in the locations where the splitting points of the cables are now placed. Therefore the lengths of the links can be summarized as is shown in Table III (a similar choice of physical topology model can be found also in [17] and in [25]).

To perform the cost evaluations we have considered WDM-PON architectures connecting the number of ONU's

included in the set: $U = (128, 512, 1024)$. These numbers derive from a technological vision. Of course in a real deployment the network has to be tailored to the actual user density, replicating the WDM PON structures if needed. We have further assumed the values in the set $w = (16, 32, 64)$ as the maximum number of multiplexed wavelengths. The maximum size of the WGR's considered has been chosen to be $M_{\max} = 64$, the minimum size being $M_{\min} = 4$. These values seem quite feasible for the present or the near-future next generation technology.

For a detailed examination of the cost evaluation results, let us consider first the case with $U = 128$ and $w = 32$. To analyze the data obtained we have grouped first the architectures by their number of stages K. Then in each group we have ordered the architectures according to increasing costs per user. The index acts as a sorting index ranking, for each K, all the architectures by the cost per user evaluated taking into account only the WGR costs.

In Fig. 15, we have taken into account only the cost due to the WGR's. This cost tends to increase with the number of stages, though this is not true in general since there are some architectures having two stages which result more expensive than others with three stages.

In Fig. 16, we instead plot only the cost due to the cables and their installation. Architectures having the same K are sorted again ranking by the cost per user including cable ad installation; then the sorted architectures are numbered with the architecture index. This time the cost does not increase monotonically with K. On the contrary it decreases starting from a minimum value assumed for $K = 5$. This behavior is due to the fact that adding more WGR stages implies sharing the cost of the longest links of the first stages by a higher number of ONU's, while the most replicated links of the network (the last links) have shorter physical lengths.

Fig. 17 shows the results when the three cost components of WGR's, cables and installation are summed. Once again the architectures are sorted by their (cable + installation + WGR) cost per user and then numbered by the index. The best performing architectures are those with $K = 3$ and, very close, those with $K = 2$. This is the result of combining the two opposite behaviors of the cables (plus installation) and the WGR costs.

In Fig. 18, we have reported the values of the maximum coarseness $(C_{\max})$ and maximum value of I $(I_{\max})$ for the architectures ordered as in Fig. 17, i.e., identified by the same architecture index used in Fig. 17. We can notice that the least expensive architectures in all the groups except for $K = 5$ are those with the smallest values of coarseness in their group. Then coarseness oscillates with the increasing of the total cost, but tends to high values. The parameter I has also an oscillating behavior with cost, but the first peaks are the highest, and then it tends to low values.

In Fig. 19 the costs are evaluated without taking into account the installation. This would be the situation when a network operator can partially reuse an already installed plant by upgrading it to a WDM-PON. We can see that, since the cable cost has a minor impact, architectures with $K = 2$ are again the best cost

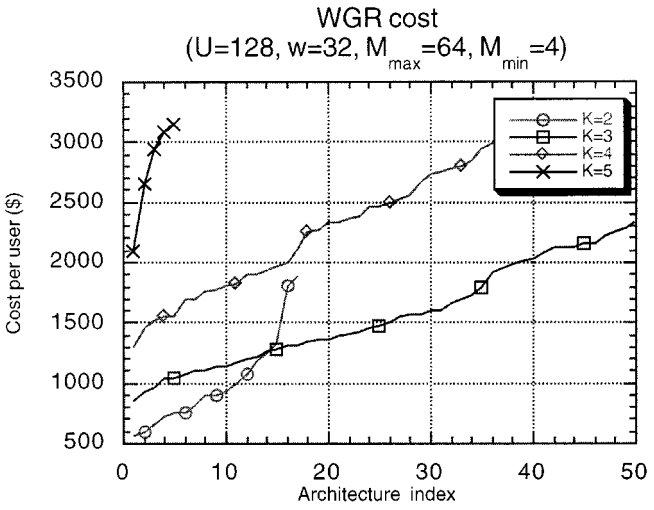

Fig. 15. WGR cost per user of the architectures obtained with $U = 128$, $w = 32$, $M_{\max} = 64$ and $M_{\min} = 4$, ordered by increasing cost.

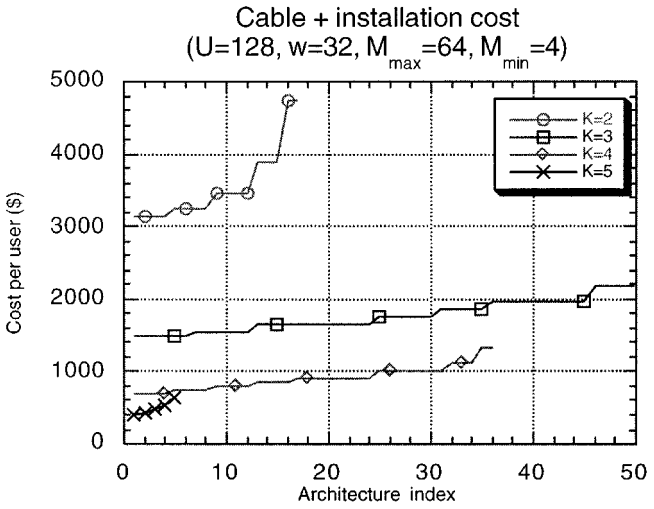

Fig. 16. Cable and installation cost per user of the architectures obtained with $U = 128$, $w = 32$, $M_{\max} = 64$ and $M_{\min} = 4$, ordered by increasing cost.

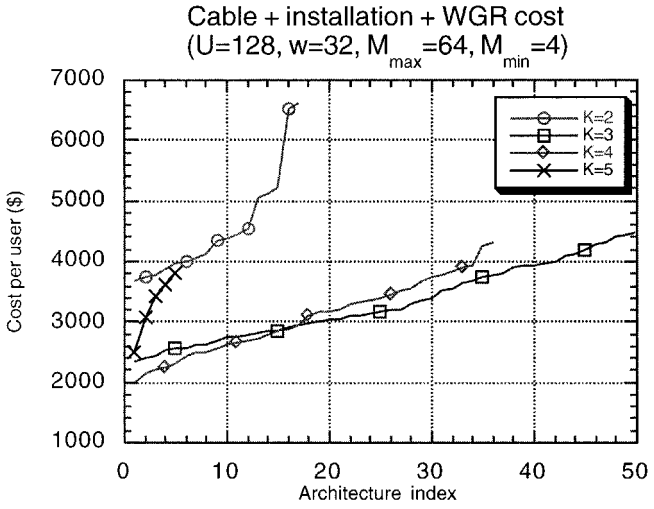

Fig. 17. Total cost per user of the architectures obtained with $U = 128$, $w = 32$, $M_{\max} = 64$ and $M_{\min} = 4$, ordered by increasing cost.

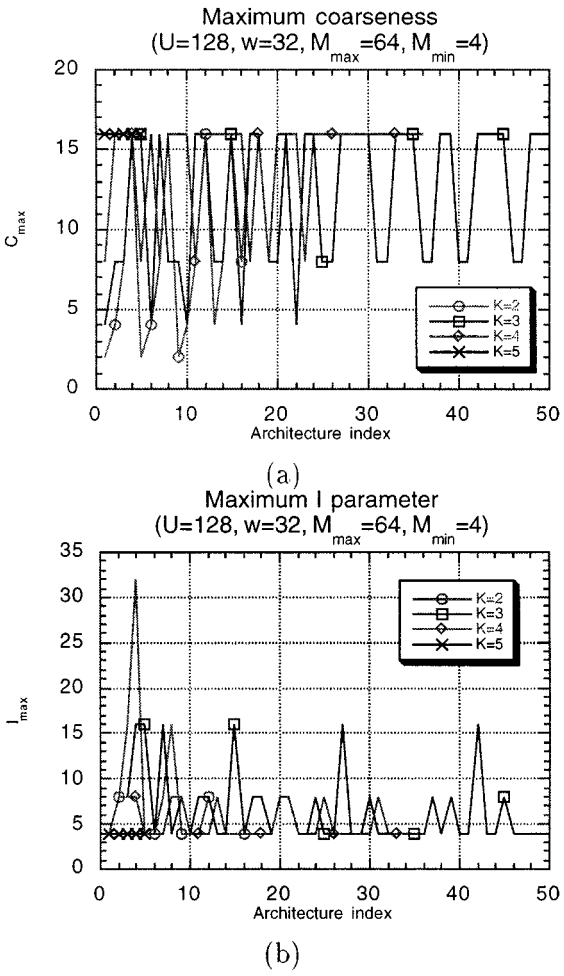

Fig. 18. Maximum values of coarseness (a) and parameter I (b) reached in the architectures obtained with $U = 128$, $w = 32$, $M_{\max} = 64$, and $M_{\min} = 4$, ordered by increasing cost.

performing, though the difference with those with $K = 3$ is small.

Finally Tables IV, V and VI give, for all the values of U and w considered, the parameters of the minimum cost architectures for each value of K.

We have reported for comparison the total cost of all these architectures (taking into account WGR's, cables and installation) and also the system margin. This last parameter has been evaluated by performing an approximate power-budget calculation. We have considered the following typical attenuation values:

- fiber attenuation: 0.2 dB/Km;
- WGR insertion loss: 6 dB;
- connectors loss: 0.3 dB;
- extra loss for channels at the limits of the passing band for WGR's with $C > 1$ (worst case): 3 dB.

We have also assumed that the power transmitted from the central office per wavelength is 0 dBm. The reported parameter, system margin, is the ratio (in dB) between the power received by each ONU and the sensitivity of the receiver, which was supposed to be –40 dBm (corresponding to the employment of a standard PIN-FET-based receiver at 622 Mbit/s).

It can be noticed from the data reported in the tables that in all the minimum cost architectures identified (having $K \leq 4$) the system margin is always above 3 dB, which is a standard limit accepted by the network designer.

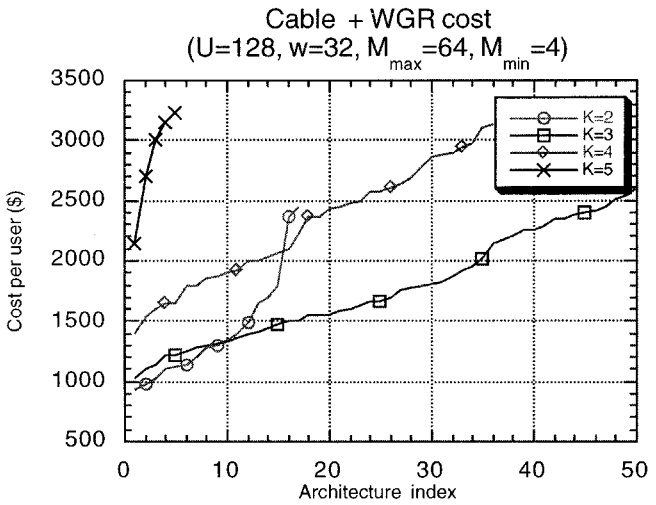

Fig. 19. Cable and WGR cost per user (without considering the installation) of the architectures obtained with $U = 128$, $w = 32$, $M_{\max} = 64$, and $M_{\min} = 4$, ordered by increasing cost.

V. WDM-PON Architectures Connectivity Map

The procedure described above to design a WDM-PON architecture with minimum cost allows us to evaluate the parameters of each network device. The procedure does not allow us, however, to understand automatically which source in the CO is connected to which ONU. The exact map of connectivity of a WDM-PON can be built by inspection, but this proves to be quite cumbersome for large amounts of ONU's and stages. For this reason we have developed a tool based on a discrete model of the network optical components that can automatically determine which of the wavelengths transmitted by the sources in the CO reaches which subscriber.

In the model, the connectivity of any WDM-PON architecture with tree topology is described by a matrix transfer function (in a similar way as in [14], but with a different formalism). In this way a given input pattern of optical WDM signals can be mapped onto the output network ports (representing the ONU's) by means of a simple matrix product.

In our model, a tree-topology based PON is partitioned in stages and interstages as shown in Fig. 20. A stage is composed of the optical devices that occupy the same level of the tree, while an interstage is composed of the optical fibers that interconnect devices belonging to two consecutive stages. Routing stages are numbered by an index k varying between 0 and K. Stage 0 corresponds to the CO, while stage K contains the WGR's directly connected to the ONU's. Interstages are also numbered from 0 to K. In this paper, as already mentioned, we will examine only the downstream connectivity, but it can be shown that our tool is able to plot also the upstream network connectivity function with limited changes.

In the model the optical channels are defined in the bidimensional domain described in Section II. We recall that an optical signal traveling through an input (output) port of a routing device is identified by two coordinates, the first belonging to a discrete spatial domain that represents the set of all the possible

TABLE IV
BEST COST PERFORMING ARCHITECTURES WITH $U = 128$, $M_{\max} = 64$ AND $M_{\min} = 4$

w	K	$\vec{M}$	$\vec{N}$	$\vec{C}$	$\vec{I}$	Per user cost ($)	System margin (dB)
16	2	[16 64]	[1 2]	[1 2]	[8 8]	3733	22.89
	3	[16 16 32]	[1 2 4]	[1 2 4]	[8 8 8]	2446	13.29
	4	[16 16 16 16]	[1 2 4 8]	[1 2 4 8]	[8 8 8 8]	2246	3.69
32	2	[8 64]	[1 2]	[1 2]	[4 4]	3697	22.89
	3	[8 8 32]	[1 2 4]	[1 2 4]	[4 4 4]	2336	13.29
	4	[8 8 8 16]	[1 2 4 8]	[1 2 4 8]	[4 4 4 4]	1991	3.69
64	2	[4 64]	[1 2]	[1 2]	[2 2]	3680	22.89
	3	[4 4 32]	[1 2 4]	[1 2 4]	[2 2 2]	2288	13.29
	4	[4 4 4 16]	[1 2 4 8]	[1 2 4 8]	[2 2 2 2]	1878	3.69

TABLE V
BEST COST PERFORMING ARCHITECTURES WITH $U = 512$, $M_{\max} = 64$ AND $M_{\min} = 4$

w	K	$\vec{M}$	$\vec{N}$	$\vec{C}$	$\vec{I}$	Per user cost ($)	System margin (dB)
16	2	[64 64]	[1 8]	[1 2]	[32 8]	3592	22.89
	3	[64 64 64]	[1 2 8]	[1 2 4]	[32 32 16]	1964	13.29
	4	[64 64 64 64]	[1 2 4 8]	[1 2 4 8]	[32 32 32 32]	1364	3.69
32	2	[32 64]	[1 8]	[1 2]	[16 4]	3570	22.89
	3	[32 32 64]	[1 2 8]	[1 2 4]	[16 16 8]	1898	13.29
	4	[32 32 32 64]	[1 2 4 8]	[1 2 4 8]	[16 16 16 16]	1211	3.69
64	2	[16 64]	[1 8]	[1 2]	[8 2]	3556	22.89
	3	[16 16 64]	[1 2 8]	[1 2 4]	[8 8 4]	1854	13.29
	4	[16 16 16 64]	[1 2 4 8]	[1 2 4 8]	[8 8 8 8]	1108	3.69

TABLE VI
BEST COST PERFORMING ARCHITECTURES WITH $U = 1024$, $M_{\max} = 64$ AND $M_{\min} = 4$s

w	K	$\vec{M}$	$\vec{N}$	$\vec{C}$	$\vec{I}$	Per user cost ($)	System margin (dB)
32	2	[64 16]	[1 64]	[1 2]	[32 1]	4195	22.89
	3	[64 64 16]	[1 2 64]	[1 2 4]	[32 32 2]	2252	13.29
	4	[64 32 32 16]	[1 4 8 64]	[1 2 4 8]	[32 16 16 4]	1558	3.69
64	3	[32 64 8]	[1 2 128]	[1 2 8]	[16 16 1]	2598	13.29
	4	[32 32 32 8]	[1 2 4 128]	[1 2 4 8]	[16 16 16 1]	1708	3.69

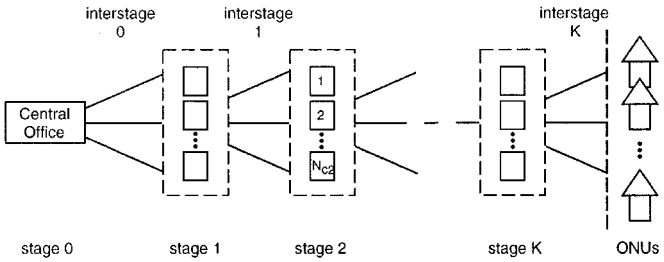

Fig. 20. Representation of the WDM-PON used by the connectivity-mapping tool.

input (output) ports of the device; the second belonging to a discrete wavelength domain representing the set of WDM channels that can be multiplexed on any port of the device.

In a similar way, these concepts are extended to the matrix model of the WDM-PON. Since there are no wavelength conversions the dimension of the wavelength domain is constant throughout the whole network, as already anticipated in Section II. It is actually equal to the maximum number w of wavelengths per link.

Two matrices are associated respectively with the signals in inputs or outputs of stage k: IN_k is a $w \times L_k$ matrix, while OUT_k is a $w \times \Sigma_k$ matrix. L_k and Σ_k define, respectively, the input and output spatial dimension of a stage. The elements of these matrices can be numbers representing a numerical label assigned to a particular channel which can be used to trace its path through the various stages. Each element of the fth row of IN_k (OUT_k) corresponds to an optical signal at wavelength f, while each element of the ith column occupies a spatial position i in the inputs (outputs) of the stage.

The algebraic relations between these matrices are determined by the spatial routing function performed on the optical signals by the devices belonging to the stage. The output matrix OUT_k is obtained by the product of the input matrix IN_k by an operator representing the kth stage connectivity function (see Fig. 21)

$$\text{OUT}_k = ST_k \cdot \text{IN}_k \quad k \in [1, K].$$

The space switching function performed by a stage over an optical signal varies according to its wavelength. Therefore, the stage operator corresponds to a three-dimensional (3-D) matrix. The fth bidimensional submatrix of the operator multiplies the fth column of the signal matrix IN_k, independently of the other columns. The result of this multiplication must be a switch in the positions of the labels representing the channels in the spatial domain, as a consequence of the routing function performed by the devices of the stage (Fig. 21).

Since the stage is a set of routing devices, its input (output) port set will include the input (output) ports of all the devices in the stage. In our case, where all the N_k devices of a stage are identical and squared with size M_k, the number L_k of input ports of a stage should be equal to the number of output ports Σ_k

$$L_k = \Sigma_k = N_k M_k \quad k \in [0, K].$$

In order to implement a model based on matrices, however, we must define stages and interstages in a different way so as to have all matrices of equal size. Since we are considering tree topologies, the maximum spatial dimension is reached always at the last stage K and is equal to the number of users U connected to the architecture. Therefore also the dimension of matrices representing the other upstream stages is chosen equal to U

$$L_k = \Sigma_k = N_K M_K = U \quad k \in [0, K].$$

Our choice has been to place the submatrices corresponding to the devices of a stage k one after the other to occupy the first rows of a matrix ST_k. The remaining rows are padded with zeros.

In the case of an interstage k, connecting the two stages k and $k+1$ (except the interstage K, which connects the stage K to the ONU's), the output matrix is IN_{k+1}, while the input is OUT_k. IN_{k+1} is obtained by the multiplication of OUT_k by an operator INT_k representing the interstage connectivity function

$$\mathrm{IN}_{k+1} = \mathrm{INT}_k \cdot \mathrm{OUT}_k \quad k \in [0, K].$$

Though the routing performed by an interstage is totally independent of the wavelengths, 3-D matrices have been employed also to represent interstages, in order to allow the matrix product.

The matrix representing the signals transmitted by the sources in the CO, indicated by IN or equivalently OUT_0, undergoes modifications (routing functions) through the various stages of the network that are represented as follows:

$$\begin{aligned}
\mathrm{OUT}_0 &= \mathrm{IN} \\
\mathrm{IN}_1 &= \mathrm{INT}_0 \cdot \mathrm{OUT}_0 \\
\mathrm{OUT}_1 &= \mathrm{ST}_1 \cdot \mathrm{IN}_1 = \mathrm{ST}_1 \cdot \mathrm{INT}_0 \cdot \mathrm{OUT}_0 \\
\mathrm{IN}_2 &= \mathrm{INT}_1 \cdot \mathrm{OUT}_1 = \mathrm{INT}_1 \cdot \mathrm{ST}_1 \cdot \mathrm{INT}_0 \cdot \mathrm{OUT}_0 \\
&\cdots \\
\mathrm{IN}_{\mathrm{ONU}} &= \mathrm{INT}_K \cdot \mathrm{OUT}_K = \mathrm{INT}_K \cdot \mathrm{ST}_K \cdot \cdots \cdot \mathrm{INT}_0 \cdot \mathrm{OUT}_0
\end{aligned}$$

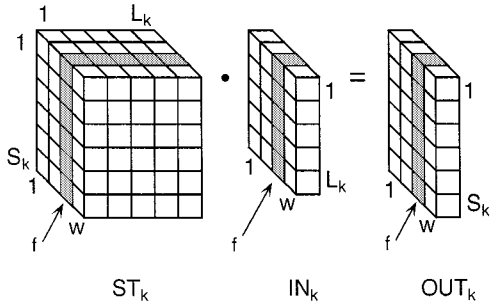

Fig. 21. Three-dimensional stage operator with its input and output matrices.

$\mathrm{IN}_{\mathrm{ONU}}$ is the matrix of the signals reaching the subscribers; it can also be written as

$$\mathrm{OUT} = \mathrm{IN}_{\mathrm{ONU}} = \mathrm{NET} \cdot \mathrm{IN}$$

NET is the operator representing the discrete transfer function (or connectivity function) of the WDM-PON architecture; it can be obtained by the product of all the stage and interstage operators

$$\begin{aligned}
\mathrm{NET} &= \mathrm{INT}_K \cdot \mathrm{ST}_K \cdot \mathrm{INT}_{K-1} \\
&\quad \cdot \mathrm{ST}_{K-1} \cdot \ldots \cdot \mathrm{ST}_1 \cdot \mathrm{INT}_0 = \prod_{i=1}^{K} \mathrm{ST}_i \cdot \mathrm{INT}_i \cdot \mathrm{INT}_0.
\end{aligned}$$

In our tool, the stage and interstage matrices are obtained automatically starting from a description of the topology and the parameters of the network devices. The various stage operators are built by assembling the operators corresponding to the routing devices they include. Though the tool is flexible and it can be used with many active and passive optical devices (such as splitters, WDM demultiplexers, amplifiers, and so on), we are interested in this paper only in WDM-PON's based on the WGR's. Therefore, we are now going to show how the 3-D matrix operator of this component is constructed starting from its routing function.

Let us assume for simplicity a number of wavelengths $w \leq M$. Let us also consider initially a router with minimum coarseness $C = 1$. The WGR matrix operator can be readily evaluated by reinterpreting (1): the position in the output matrix of a channel having a given wavelength and a given input position is obtained by a circular shift. The entity of this shift depends on the wavelength index: in fact the shift must be of $f - 1$ positions if the wavelength is f. The examples of routing reported in Fig. 5 of Section II could be helpful to visually verify this behavior.

Therefore, the 3-D operator of the WGR must be composed of w bidimensional $M \times M$ matrices, each of which algebraically performs a circular shift on the elements of the corresponding row in the input matrix IN. We call $\mathrm{SHIFT}_{[n]}$ a matrix performing an order n shift. For example the matrix corresponding to $f = 1$ is $\mathrm{SHIFT}_{[0]}$ (identity matrix), the matrix corresponding to $f = 2$ is $\mathrm{SHIFT}_{[1]}$, the matrix corresponding to f is $\mathrm{SHIFT}_{[f-1]}$. The overall 3-D matrix associated to a WGR 6×6, with $C = 1$ and $w = 4$, is represented in Fig. 22.

The figure also shows the shift submatrices composing the operator.

If the number w of wavelengths is greater than the number M of WGR terminations, the wavelengths exceeding M must be cyclically routed, according to the WGR routing property. To do this the first block of M shift matrix is identically repeated along the wavelength dimension to compose the operator [see Fig. 23(a)]. Thus, a shift matrix $\text{SHIFT}_{[f \bmod M-1]}$ corresponds to wavelength f. Finally, in the general case of coarseness $C > 1$ the three-dimensional matrix can be built by replicating C times each shift matrix of the corresponding WGR operator with coarseness $C = 1$ [see Fig. 23(b)].

A bidimensional approach has been adopted in the following application of the model to simplify the calculus of every matrix and the product between 3-D matrices. Though the model of the WDM-PON networks defined so far is based on 3-D operators, the actual computations are made by the tool employing an equivalent bidimensional data structure. All the submatrices $U \times U$ of a stage or an interstage operator $U \times U \times w$ are sequentially placed on the main diagonal of a bidimensional matrix $(w \cdot U) \times (w \cdot U)$ [Fig. 24(a)]. Outside the diagonal, all matrix elements are null. Analogously all the rows of an IN or OUT $U \times w$ signal matrix are sequentially placed in a vector with dimensions $(w \cdot U) \times 1$ [Fig. 24(b)].

The matrices obtained, though very big in dimensions, are actually sparse, with only few nonzero elements. Therefore the computational complexity is in no way increased by this bidimensional representation, while the data representation complexity is diminished compared to the use of actual three-dimensional data structures.

To show how our tool works we have applied it to the minimum cost architectures identified in Section IV with $U = 128$, $w = 32$, $M_{\max} = 64$ and $M_{\min} = 4$, with respectively $K = 2$, $K = 3$ and $K = 4$ stages. The architectures are shown in Figs. 25–27.

In Fig. 28, the connectivity of the architectures evaluated by the tool can be seen. It can be noticed that each ONU receives a channel at a particular wavelength and that at the same time wavelength reuse is implemented.

VI. Critical Issues

In this section, we would like to comment on some critical issues concerning the technological feasibility of the proposed solutions of IC WDM-PON's.

The first consideration concerns the WGR devices. The size of the WGR's is not an issue any more, since 64×64 integrated routers are already off-the-shelf commercial products and larger devices (e.g., 128×128) exist as experimental prototypes and will probably soon be on the market. It is likely that WGR costs will decrease in the future as more and more of these devices will be produced.

The coarseness instead is a critical parameter. As we anticipated in Section II, the transfer function of a coarse WGR must have a flat shape in the passing bands and sharp transitions from the attenuated to the passing regions. Various techniques have been developed to obtain a flattened band, especially with the purpose of reducing the sensitivity of the router to carrier

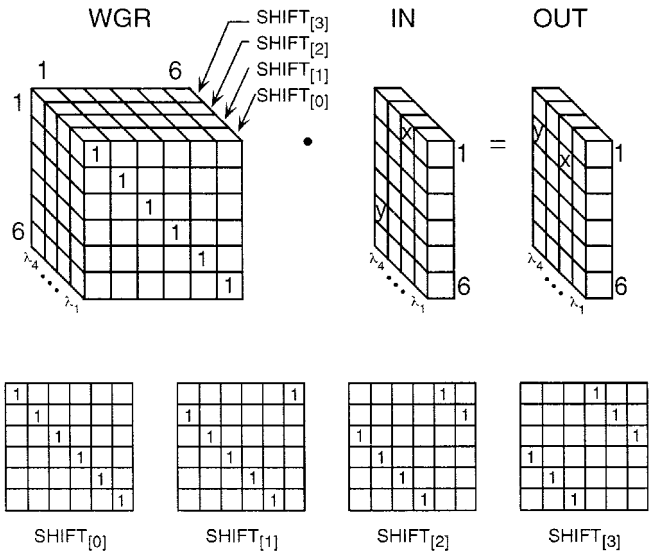

Fig. 22. Three-dimensional operator associated to a WGR 6×6 with $C = 1$ for $w = 4$.

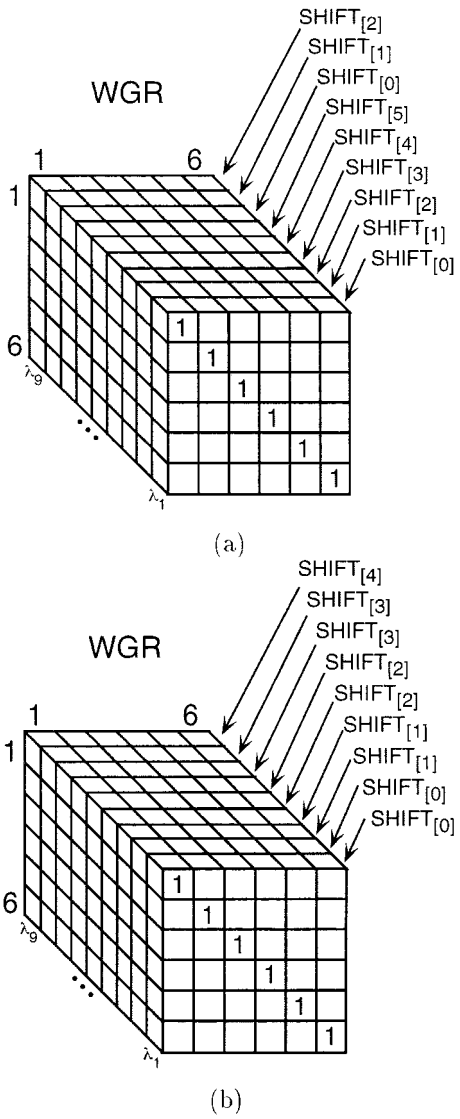

Fig. 23. Three-dimensional operator associated, for $w > 6$, to a WGR 6×6 and with: (a) $C = 1$ and (b) $C = 2$.

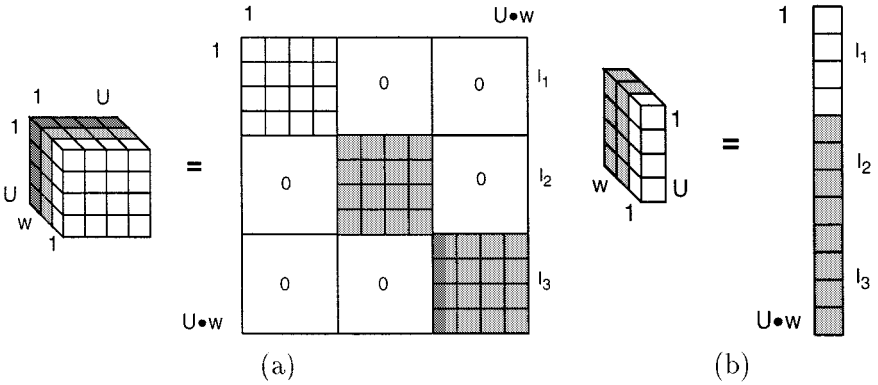

Fig. 24. Equivalence between the 3-D and 2-D representation of the network connectivity operators NET (part a) and IN or OUT (part b).

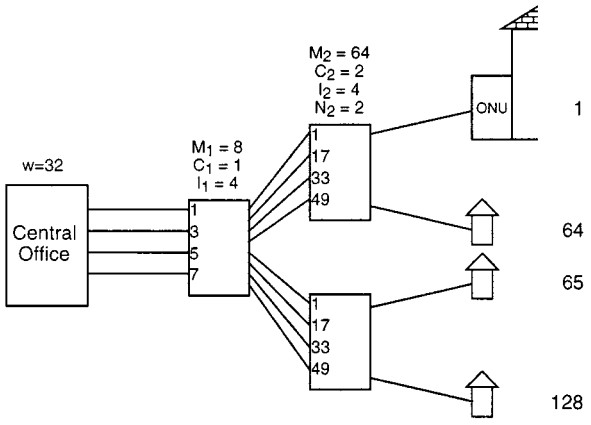

Fig. 25 Minimum cost two-stage architecture with $U = 128$, $w = 32$, $M_{\max} = 64$, and $M_{\min} = 4$.

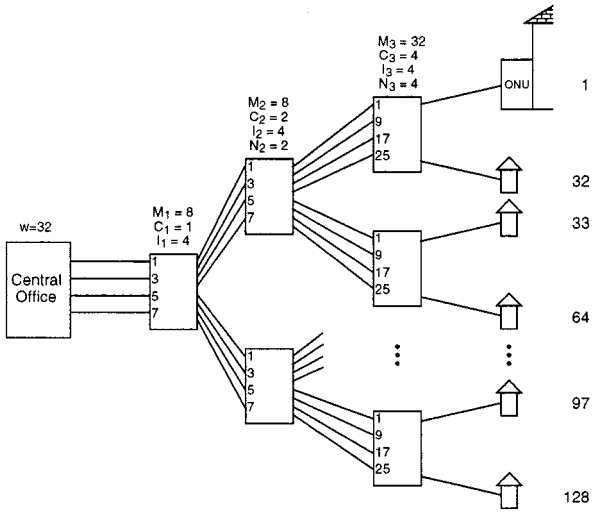

Fig. 26. Minimum cost three-stage architecture with $U = 128$, $w = 32$, $M_{\max} = 64$, and $M_{\min} = 4$.

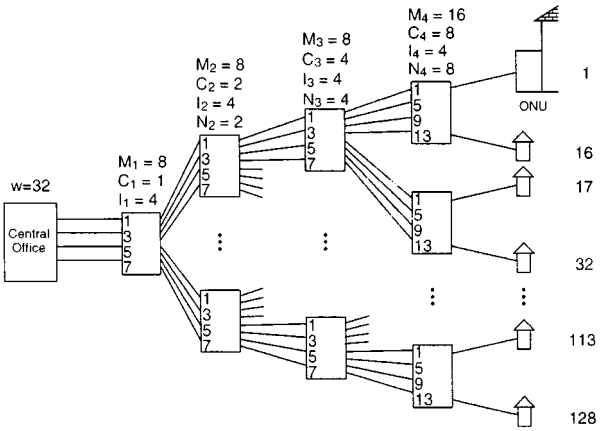

Fig. 27. Minimum cost four-stage architecture with $U = 128$, $w = 32$, $M_{\max} = 64$, and $M_{\min} = 4$.

wavelength fluctuations ([36]–[39]). Methods to obtain sharp transitions have also been proposed ([23], [40]–[42]). The main techniques that would be useful to our architectures comprise: multiple-Rowland-circle design [38], spatial filtering obtained by introducing attenuation and phase-shifts in the WGR arms [43], employment of multimode-interference couplers [44], employment of "macro-WGRs" obtained by cascading two WGR's and connecting them with waveguides [45], etc. Commercial products guarantee a full-width at half-maximum (FWHM) to channel-spacing ratio of 60%, which corresponds to a coarseness $3 < C < 4$. The same values may also be inferred from the data reported in recent theoretical studies such as [46]. It is our feeling that in the future, a coarseness $C = 8$ could be achieved by a careful and on-purpose device design, maybe paying the price of an increase of the WGR total insertion loss.

Another issue regarding the WGR's in a WDM PON concerns the thermal stability. Techniques have been developed for a single-stage network employing space division RiteNet-like bidirectionality which exploit the optical feedback provided by the upstream channels to control the temperature of the sources in the CO according to the temperature variations in the RN [47], [50]. This approach would be difficult to implement with multistage networks. An alternative method proposed in [48], in which the WGR's are equipped with heaters instead of coolers, could work well also with multistage networks. However in this case the passive characteristics of the network is lost and each remote router must be supplied with the power required by the heaters and by its control electronics. Other solutions are proposed in [49], [22].

A further cause of impairment for the network could derive from the fact that the FSR is not constant, but varies as the distance of a wavelength channel form the central wavelength of

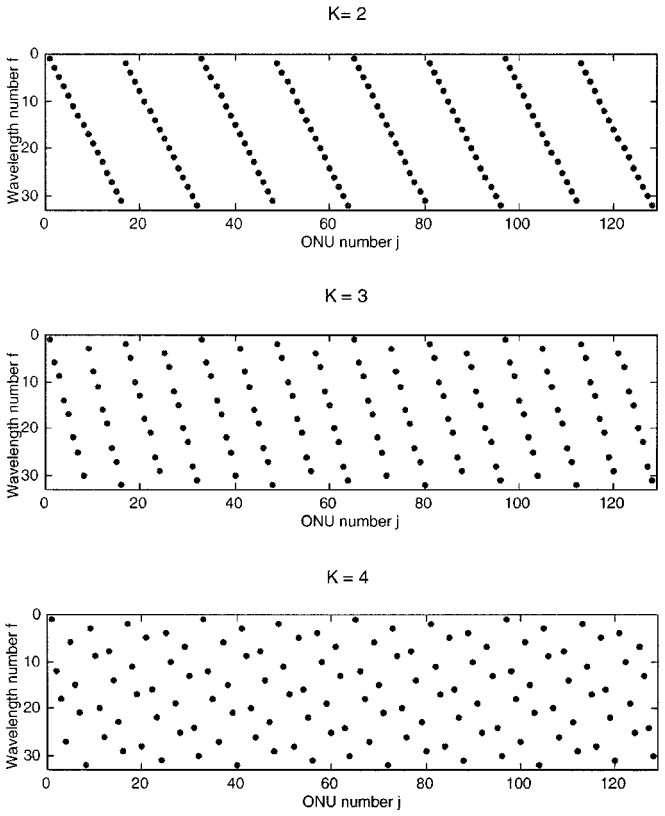

Fig. 28. Connectivity of the architectures represented in Figs. 25–27.

the device increases. The FSR (in frequency) is in fact proportional to the inverse of the group index of the waveguide mode, which depends on the frequency [12]. A specific WGR design approach has been presented [52] to reduce this problem for WGR's used as $N \times N$ routers. With this design also the in loss of the outer channels of the WGR compared to the inner ones [12] is reduced.

Dispersion introduced by optical devices could be a problem in high-density WDM systems in which channel spacing reduces. The WGR in theory is not a dispersive device; in reality, process variations can lead to amplitude and phase errors in the waveguide array which may affect the dispersion [53]. Recently published measurements [53], [54] however, indicate that for standard WGR's (coarseness $C = 1$) the dispersion over the passing band is very low, and lower than that of other technologies.

Finally we would like to point out that many other elements could be added to our analysis in further developments. For example we did not consider the cross-talk between channels or the effect of the temperature fluctuations on the quality of signals, since we preferred to look closer to the connectivity functions. Also, in our cost analysis we did not include the costs of the active components (sources, modulators and receivers), as our purpose was to compare networks only on the basis of their passive optical hardware. WGR nonideality such as dispersion and the nonuniformity of the free spectral range should also be further investigated.

We would like to notice, however, that the design principles regarding the network connectivity we found remains valid regardless of all the possible implementation issues. Moreover, the algorithm to generate the network parameters and the tool we developed to map the connectivity are quite flexible instruments and could be upgraded with minor changes to take into account most of the aspects that were not considered in this first work.

VII. Conclusion

In this work, we presented a study on multistage WDM passive optical networks employing WGR's as basic optical routing components. A theoretical analysis of the connectivity properties allowed us to identify a family of architectures in which an efficient implementation of wavelength reuse allows us to reach a high number of connected users. A cost-comparison has been performed in order to find the optimum parameter dimensioning for the architectures proposed. The power-budget and technological feasibility of these architectures have also been discussed. By this approach we could identify the minimum cost WDM-PON networks with two, three, and four stages, for various numbers of connected users ranging from 16 to 1024. The results obtained show that these architectures are feasible given the present development of the optical technology. Furthermore the costs tend to decrease when the number of stages increases, though this is accompanied by a reduction of the system margin. Finally, in this work we have also proposed a model based on a matrix representation of the WGR routing function and of the network connectivity. A design tool developed based on this model allows us to automatically compute the route of each wavelength- channel through the network: this can be helpful to better understand the properties of the multistage WDM PON's and therefore possibly to study and propose new architectures.

References

[1] N. Frigo, "Local access optical networks," *IEEE Network Mag.*, vol. 10, pp. 32–36, Nov./Dec. 1996.
[2] C. Dragone, "An $N \times N$ optical multiplexer using a planar arrangement of two star couplers," *IEEE Photon. Technol. Lett.*, vol. 3, pp. 812–815, Sept. 1991.
[3] N. Frigo *et al.*, "A wavelength-division multiplexed passive optical network with cost-shared components," *IEEE Photon. Technol. Lett.*, vol. 6, pp. 1365–1367, Nov. 1994.
[4] M. Zirngibl *et al.*, "LAR-Net, a local access router network," *IEEE Photon. Technol. Lett.*, vol. 7, pp. 215–217, Feb. 1995.
[5] N. Frigo and P. Iannone, "Multiple star, passive optical network based on remote interrogation of terminal equipment,", July 1997. EP 0 782 285 A2.
[6] Y. Tachikawa and K. Okamoto, "Arrayed-waveguide grating lasers and their applications to tuning-free wavelength routing," *Inst. Elect. Eng. Proc Optoelectron.*, vol. 143, no. 5, pp. 322–328, Oct. 1996.
[7] H. Takahashi *et al.*, "Transmission characteristics of arrayed waveguide $N \times N$ wavelength multiplexer," *J. Lightwave Technol.*, vol. 13, pp. 447–455, Mar. 1995.
[8] C. Dragone, C. Edwards, and R. Kistler, "Integrated optics $N \times N$ multiplexer on silicon," *IEEE Photon. Technol. Lett.*, vol. 3, pp. 896–899, Oct. 1991.
[9] C. Dragone, "Efficiency of a periodic array with nearly ideal element pattern," *IEEE Photon. Technol. Lett.*, vol. 1, pp. 238–240, Aug. 1989.
[10] C. Dragone *et al.*, "Efficient multichannel integrated optics star coupler on silicon," *IEEE Photon. Technol. Lett.*, vol. 1, pp. 241–243, Aug. 1989.
[11] B. Glance, I. Kaminow, and R. Wilson, "Applications of the integrated waveguide grating router," *J. Lightwave Technol.*, vol. 12, pp. 957–962, June 1994.
[12] A. van Dam, "InP-based polarization independent wavelength demultiplexers," Ph.D dissertation, Delft Univ. Technol., 1997.

[13] M. Smit and C. van Dam, "PHASAR-based WDM-Devices: Principles, design and applications," *IEEE J. Select. Topics Quantum Electron.*, vol. 2, pp. 236–250, June 1996.
[14] K. Oguchi, "New notations based on the wavelength transfer matrix for functional analysis of wavelength circuits and new WDM networks using AWG-based star coupler with asymmetric characteristics," *J. Lightwave Technol.*, vol. 14, pp. 1255–1263, June 1996.
[15] R. Barry and P. Humblet, "Latin routers, design and implementation," *J. Lightwave Technol.*, vol. 11, pp. 891–899, May/June 1993.
[16] Y. Lin and D. Spears, "Passive optical subscriber loops with multiaccess," *J. Lightwave Technol.*, vol. 7, pp. 1769–1777, Nov. 1989.
[17] S. Wagner and H. Lemberg, "Technology and system issues for a WDM-based fiber loop architecture," *J. Lightwave Technol.*, vol. 7, pp. 1759–1768, Nov. 1989.
[18] P. Iannone, K. Reichmann, and N. Frigo, "Wavelength-dependent modulation effects of light-emitting diodes in multiple-subband passive optical networks," in *OFC '98 Tech. Dig.*, pp. 401–403.
[19] N. Frigo *et al.*, "Approaches to multiple service delivery over passive optical networks," in *OFC '98 Tech. Dig.*, pp. 404–405.
[20] P. Smith, D. Faulkner, and G. Hill, "Evolution scenarios for optical telecommunication networks using multiwavelength transmission," *Proc. IEEE*, vol. 81, pp. 1580–1587, Nov. 1993.
[21] M. Gagnaire, "An overview of broad-band access technologies," *Proc. IEEE*, vol. 85, pp. 1958–1972, Dec. 1997.
[22] M. Parker *et al.*, "Passband-flattened arrayed-waveguide grating featuring a new aspheric output star coupler," in *Proc. NOC'98*, vol. III, pp. 122–125.
[23] C. Dragone, "Frequency routing device having a wide substantially flat passband,", May. no. 5 412 744.
[24] M. van Deventer *et al.*, "Evolutional phases to an ultra-broadband access network: Results from ACTS-PLANET," *IEEE Commun. Mag.*, vol. 35, pp. 72–77, Dec. 1997.
[25] N. Andersen *et al.*, "Broadbandloop : A full-service access network for residential and small business users," *IEEE Commun. Mag.*, vol. 35, pp. 88–93, Dec. 1997.
[26] A. Tan, "SUPER PON—A fiber to the home cable network for CATV and POTS/ISDN/VOD as economical as a coaxial cable network," *J. Lightwave. Technol.* , vol. 15, pp. 213–218, Feb. 1997.
[27] A. Koonen *et al.*, "HDWDM upgrade of CATV fiber-coax networks for broadband interactive services," in *Proc. ECOC'96*, p. WeB. 1.3.
[28] U. Hilbk *et al.*, "Experimental WDM upgrade of a PON using an arrayed waveguide grating," in *Proc. ECOC'96*, p. WeB. 1.5.
[29] R. Menendez, S. Wagner, and H. Lemberg, "Passive fiber-loop architecture providing both switched and broadcast transport," *Electron. Lett.*, vol. 26, no. 5, pp. 273–274, Mar. 1990.
[30] B. Glance *et al.*, "A single-fiber WDM local access network based on amplified LED transceivers," *IEEE Photon. Technol. Lett.*, vol. 8, pp. 1241–1242, Sept. 1996.
[31] C. Giles *et al.*, "Single-fiber access PON using downstream 1550 nm WDM routing and upstream 1300 nm power combining through a fiber-grating router," in *Proc. ECOC'96*, p. WeB. 1.4.
[32] P. Iannone, N. Frigo, and T. Darcie, "WDM passive-optical-network architecture with bidirectional optical spectral slicing," in *Proc. OFC'95*, p. TuK2.
[33] N. Frigo *et al.*, "Mixed-format signal delivery and full-duplex operation in a WDM PON with a single shared source," in *Proc. OFC'95*, p. TuK5.
[34] P. Iannone, K. Reichmann, and N. Frigo, "Broadcast digital video delivered over WDM passive optical networks," *IEEE Photon. Technol. Lett.*, vol. 8, pp. 930–932, July 1996.
[35] P. Iannone *et al.*, "Simultaneous WDM and broadcast transmission using a single multiwavelength waveguide-grating-router laser," *IEEE Photon. Technol. Lett.*, vol. 8, no. 10, pp. 1397–1399, Oct. 1996.
[36] L. Spiekman *et al.*, "Polarization-independent InP-based phased-array wavelength demultiplexer with flattened wavelength response," in *Proc. ECOC'94*, pp. 759–762.
[37] D. Touchet *et al.*, "Passband flattening of PHASAR WDM using input and output star couplers designed with two focal points," in *Proc. OFC'97*, p. ThM7.
[38] Y. Ho, H. Li, and Y. Chen, "Flat channel-passband-wavelength multiplexing and demultiplexing devices by multiple-Rowland-circle design," *IEEE Photon. Technol. Lett.*, vol. 9, pp. 342–344, Mar. 1997.
[39] K. Okamoto, K. Takiwuchi, and Y. Homori, "Eight-channel flat spectral response arrayed-waveguide multiplexer with asymmetrical machzehnder filters," *IEEE Photon. Technol. Lett.*, vol. 8, pp. 373–374, Mar. 1996.
[40] M. Amersfoort *et al.*, "Passband broadening of integrated arrayed waveguide filters using multimode interference couplers," *Electron. Lett.*, vol. 32, no. 5, pp. 449–451, Feb. 1996.
[41] H. Uetsuka *et al.*, "Recent improvements in arrayed waveguide grating dense wavelength division multi/demultiplexers," in *Proc. ECIO'97*, Paper EWC4.
[42] A. Rigny, A. Bruno, and H. Sik, "Double-phased array for a flattened spectral response," in *Proc. ECOC'97*, pp. 79–82.
[43] C. Dragone *et al.*, "Waveguide grating router with maximally flat passband produced by spatial filtering," *Electron. Lett.*, vol. 33, no. 15, pp. 1312–1314, July 1997.
[44] M. Amersfoort *et al.*, "Passband broadening of integrated arrayed waveguide filters using multimode interference couplers," *Electron. Lett.*, vol. 32, no. 15, pp. 449–451, Feb. 1996.
[45] C. Dragone, "Frequency routing device having a wide substantially flat passband,", Jan. 1996. no. 5 488 680.
[46] C. Dragone, "Efficient techniques for widening the passband of a wavelength router," *J. Lightwave Technol.*, vol. 16, pp. 1895–1906, Oct. 1998.
[47] D. Mayweather *et al.*, "Wavelength tracking of a remote WDM router in a passive optical network," *IEEE Photon. Technol. Lett.*, vol. 8, pp. 1238–1240, Sept. 1996.
[48] S. Kobayashi *et al.*, "High operation temperature 1×8 AWG modules for dense WDM applications," in *Proc. ECIO'97*, p. EWC5.
[49] Y. Inoue *et al.*, "Athermal silica-based arrayed-waveguide grating (AWG) multiplexer," in *Proceedings of ECIO'97*, p. TH3B.
[50] R. Monnard *et al.*, "Demonstration of a 12×155 Mb/s WDM PON under outside plant temperature conditions," *IEEE Photon. Technol. Lett.*, vol. 9, pp. 1655–1657, Dec. 1997.
[51] A. Luvison *et al.*, La rete di distribuzione per telecomunicazioni, Torino, 1993. Italian language, Edizioni CSELT.
[52] K. Okamoto,, "Functional planar waveguide devices," in *Optic. Networking*, A. Bononi, Ed., pp. 129–140.
[53] B. Fondeur, R. Cella, and C. Nicolas, "Effect of process variations on arrayed waveguide grating dispersion," in *Proc. ECOC'99*, vol. I, pp. 328–329.
[54] J. Gehler and K. Lösch, "Dispersion measurement of arrayed waveguide gratings by fourier-transform spectroscopy," in *Proc. ECOC'99*, vol. I, pp. 368–369.

Guido Maier received the Laurea degree in electronic engineering from the University "Politecnico di Milano," Milan, Italy, in 1995. Since 1997, he has been pursuing the Ph.D. degree in electronic and telecommunication engineering at "Politecnico di Milano."

In 1996, he joined CoreCom, Milan, as a Researcher, where he is now the Head of the Optical Network Laboratory. His main areas of interest are optical network modeling, design and simulation, photonic ATM and WDM switching architectures, and optical access networks.

Mario Martinelli received the Laurea degree (cum laude) in nuclear-electronic engineering from Politecnico di Milano, Italy, in 1976.

He is the Director of CoreCom, Milan, a research consortium between Politecnico di Milano and Pirelli Cavi e Sistemi, whose main area of activity is in the field of Optical Processing and Photonic Switching. In 1978, he joined the Quantum Electronics Department of CISE Advanced Technologies, Milan, where in 1986, he was appointed Head of the Coherent Optics Section. In 1992, he has been appointed Associated Professor of Optics Communications by Politecnico di Milano, where he activated the Italian first course on the subject, and in 1993 founded the Photonic Lab at the Elctronics and Information Department. He was author and coauthor of over 110 publications on the major international journal and conferences proceedings. Moreover, he holds over 20 international patents in the field of the optics and photonics technologies.

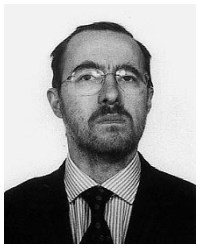

Achille Pattavina (M'85–SM'93) received the degree in Dr. Eng. degree in electronic engineering from the University "La Sapienza" of Rome, Italy, in 1977.

He was with the same university until 1991 when he moved to the Politecnico di Milano, Milan, Italy, where he is now a Full Professor. In the last ten years, he has been involved in researches on the design and performance evaluation of fast packet switching architectures for broad-band networks. He has been author of more than 80 papers in the area of communications networks published in international journals and conference proceedings. He has been author of the book *Switching Theory, Architectures and Performance in Broadband ATM Networks* (New York: Wiley). His current research interests are in the area of optical networks and wireless.

Dr. Pattavina has been a Co-Guest Editor of Special Issues on ATM Switching Systems for B-ISDN for the IEEE JOURNAL ON SELECTED AREAS IN COMMUNICATIONS and the *IEICE Transactions on Communications*. He has been Editor for Switching Architecture Performance of the IEEE TRANSACTIONS ON COMMUNICATIONS since 1994 and Managing Editor of the *European Transactions on Telecommunications* since 1997. He is a Senior Member of the IEEE Communications Society.

Elio Salvadoriwas born in Trento, Italy, in 1971. He received the degree in telecommunication engineering from the Politecnico di Milano, Milan, Italy, in 1997.

In 1996 he joined CoreCom, Milan, working on the applicability of WDM techniques in the optical access networks. From 1998 to 1999, he worked at Pirelli Optical Systems, where he has continued to develop his interest in optical networking for transport network applications. Currently, he is with Nokia Networks in the area of access networks.